Paper "Atmospheric changes caused by galactic cosmic rays over the period 1960-2010"
by C. H. Jackman et al.

Here are our Responses to the Comments by Referees #1 and #2.

Reply to Referee #1
We thank Referee #1 for helpful comments and suggestions. The "Referee's Comments" are noted first and then we give our "Reply:" to the comment.

Referee 1: **Anonymous Referee #1**
Received and published: 16 December 2015

Referee #1 *The paper studies, in the framework of the set of models involved, the effect of GCR variability on the Earth's atmosphere. The topic is important, and the authors make a strong effort in assessing the effect. The paper would be worth publishing in ACP, but this reviewer has some specific comments on the models used. The authors use the NAIRAS model for GCR modulation, based on the Badhwar-O'Neill approach, which computes the GCR spectrum on the top of the atmosphere. This spectrum is further applied for computations of the ion-production rate (IPR) in the atmosphere, using the NZETRN code, which is based on a solution of Boltzman equations to simulate transport of the nucleonic component of the cosmic-ray induced atmospheric cascade in the atmosphere. It is noteworthy that the NZETRN code was primarily designed for computations of the radiation dose, which is mostly defined by the nucleonic component of the cascade, reasonably described by the Botlzman equation approach. However, this approach neglects muon and electromagnetic branches of the cosmic ray induced cascade, which contribute essentially to ionization, especially in the lower atmosphere: for example, the electromanetic component dominates atmospheric ionization in the range between 10 and 25 km (see Fig. 11 of Bazilevskaya et al., SSR, 2008; Mishev & Velinov, JASTP, 2010, Fig. 2). This shortcoming is well realised at NASA (see, e.g., Heinbockel et al., NASA/TP-2009-215560 report, 2009): "It should also be emphasized that HZETRN does not transport certain particles such as pions, muons, positrons, electrons, and photons. These particles are used in calculating dose and dose equivalent by HETC-HEDS and FLUKA, but not HZETRN. The contribution of these particles to dose and dose equivalent values can be significant." Accordingly, this approach may lead to significant distortion of the ionization pattern as discussed below. A modern way to calculate GCR-related ionization is based on a full Monte-Carlo simulation of the atmospheric cascade (e.g., PLANETOCOSMICS, Desorgher et al., 2005; CRAC:CRII, Usoskin et al., 2006; or similar models – Atri et al., 2010; Mishev and Velinov, 2014).*

The authors are requested either to use an appropriate model or to explain specific questions raised below about the validity of the used model:

Referee #1 *- 1) As one can see in Fig.1, the ionization maximum is modeled to occur at the height of ~5 km at the equator and ~10 km in polar regions. This is unrealistically*

low. The ionization maximum (related to the Pfotzer maximum) is typically at 10 (equator) to 15- 18 (polar) km heights, according to both measurements and models, see, e.g., Fig.2. of Bazilevskaya et al. (2008) or Fig.2 in Calogovic et al. (2010), or Fig.4 of Mishev and Velinov (2014). Interestingly, the results shown by Mertenes et al. (2013, Fig. 12) for the dose rate computed by NAIRAS/HZETRN are reasonable, suggesting that it is only IPR, which is not correct, probably because of neglecting muon and electromagnetic components.

Authors' Reply to 1): The offset in the height of the maximum in GPIR is likely due to the lack of pion-initiated electromagnetic cascade processes in HZETRN 2010, the version currently implemented in NAIRAS. A comparison of NAIRAS GPIR with results from Usoskin et al. (2010) are now included in the manuscript (see new Figure 3, shown and described below), with a discussion of the differences. The new 2015 version of HZETRN will soon be integrated into NAIRAS, which includes the pion-initiated electromagnetic cascade processes.

***Referee #1** - 2) Another concern is about the North-South asymmetry. Figure 2 shows ionization at South and North poles. One can see that ionization at the S-pole is 15 % higher (at least at the height of 10 km) than at the N-pole. The same feature of N-S-asymmetry is observed also in Fig.1. This feature is not intuitively expected and is not shown by other models (e.g., Planetocosmics – see Calogovic et al., 2010). Moreover, dose rate profiles shown by Mertens et al. (2013) are perfectly symmetric as expected. Can the authors explain why GCR-related ionization is systematically higher in the S-hemisphere than in the N-hemisphere? Is it related to systematically different density profiles of the atmosphere?*

Authors' Reply to 2): The hemispheric asymmetry is due to a systematic North-South difference in the NCEP atmospheric profiles. This point has been added to the discussion of Figure 2 in the manuscript (see below).

***Referee #1** - 3) As one can see in Fig.8d, the maximum of ionization during the year 1976-77 was the highest for the entire interval (equal to that of 2009). This disagrees with observations of GCR intensities, where the 1976-77 maximum was the lowest (or equal to those in 1987 and 1997, but significantly lower than 1965 and 2009). To illustrate it, Figure A (of this report) shows the variability of the count rates of the four NMs used as an input for NAIRAS model (Mertens et al., 2013). It is unclear how the profile, shown in Fig.8d, can be obtained from this input. The authors need to explain this.*

Authors' Reply to 3): The GPIR is only slightly greater in 1977 compared to 2008, by roughly 0.03 cm^{-3} s^{-1}. This is consistent with the results shown in Mertens et al. (2013). The dose rates at zero cutoff rigidity for 2008 are still within the standard deviation of the corresponding solar minimum average dose rates (Figures 8 and 9 of Mertens et al., 2013). It was also discussed in Mertens et al. (2013) that widely

accessible GCR environmental models, such as BON10 used in NAIRAS, failed to reproduce the amount of increased heavy-ion GCR flux observed during the deep minimum between solar cycle 23 and solar cycle 24. The paucity of GCR proton and alpha measurements during this period made model comparisons unreliable for these ions.

Referee #1 *- 4) The authors state (page 33935, lines 12-16) that the approach was verified against data by Neher (1967) and the PLANETOCOSMICS model (Calogovic et al. (2010) and Gronoff et al. (2015)), but this statement is confusing. First, this reviewer cannot understand how the present result was compared with the data of direct measurements by Neher (1967), since the latter depict the maximum ionization at the height of 10/15 km for equator/poles, which disagrees with Fig.1 of this work. It is unclear how the present model can be in agreement with Calogovic et al. (2010) since the present Fig.1 disagrees with Fig. 2 of Calogovic et al., which shows the maximum of ionization at ~15 km and ~10 km in polar regions and equator, respectively (see item 1 above). Comparison with Gronoff et al. cannot be applied here since that paper deals with the thin Martian atmosphere where the atmospheric cascade is not fully developed and the difference between NZETRN and appropriate models is unimportant.*

Authors' Reply to 4): The Neher data is referenced to one atmospheric density value. Scaling the Neher data to the real atmospheric density changes the altitude of the maximum ionization rate. The comparison with Calogovic et al. was with respect to qualitative features and the range in the maximum ionization rates. At any rate, this section of the manuscript has been removed. Instead, explicit comparisons of NAIRAS GPIR with the results of Usoskin et al. (2010) are shown, and the differences are discussed.

Authors' modification of Paper as a result of specific questions 1), 2), 3), and 4): The revised Section 2 of the manuscript now reads:

Section 2: NAIRAS GCR ionization rate

The Nowcast of Atmospheric Ionizing Radiation for Aviation Safety (NAIRAS) team at NASA Langley Research Center (see http://sol.spacenvironment.net/~nairas/) has developed and integrated a model to include GCRs into their ionizing radiation computation. The interplanetary magnetic field varies over a solar cycle and provides a modulation of the GCR spectral flux, which has been referred to as a solar modulation potential (e.g., Badhwar and O'Neill, 1996). For real-time application of the NAIRAS model, four high-latitude, ground-based neutron monitor count rate measurements are used to cross correlate with the solar modulation potential and provide the NAIRAS model's GCR spectral flux incident on the Earth for penetration into and through the atmosphere. NAIRAS is a physics-based model that maximizes the use of measurement input data (Mertens et al., 2013, and references therein).

In the NAIRAS model, GCRs are transported from outside the heliosphere to 1 AU by the Badhwar and O'Neill (1992, 1994, 1996) and O'Neill (2010) NASA model, with the solar modulation potential determined from measurements of ground-based neutron monitor count rates. The GCR spectral flux at 1 AU travel through the

magnetosphere by means of a transmission factor determined by the vertical geomagnetic cutoff rigidity computed in the International Geomagnetic Reference Field (IGRF) model (Finlay et al., 2010). The vertical cutoff rigidities are determined by numerical solutions of charged particle trajectories in the IGRF field using the techniques advanced by Smart and Shea (1994, 2005). After transmission through the magnetosphere, the GCR spectral flux travels through the neutral atmosphere using the NASA HZETRN deterministic transport code (Mertens et al., 2012). The global distribution of atmospheric mass density is obtained from NCAR/NCEP Reanalysis 1 data at pressure levels larger than 10 hPa (Kalnay et al., 1996) and the Naval Research Laboratory Mass Spectrometer and Incoherent Scatter model atmosphere data at pressure levels less than 10 hPa (Picone et al., 2002).

The NAIRAS model has been used to compute the annual average GCR-produced ionization rates (GPIR) for the 1960–2010 time periods. For these time periods, measurements from the Thule and Izmiran neutron monitor stations were used to determine the solar modulation potential. GPIR in the NAIRAS model are computed by multiplying the dose rate in air by the atmospheric density, divided by 35 eV per ion-pair. The annual average GPIR from the NAIRAS model for two years, 2002 and 2009, are presented in Fig. 1. This shows the inverse relationship between GPIR and solar activity. Year 2002 is very close to solar maximum and shows a smaller GPIR with maximum ionization rates of nearly 15 cm^{-3} s^{-1}, whereas year 2009 is very close to solar minimum with about a factor of two larger maximum ionization rate of 30 cm^{-3} s^{-1}. The time-dependent variation in the GPIR at 90S and 90N is given in Fig. 2. Peaks in GPIR occur in 1965, 1977, 1987, 1997, and 2009, reflective of solar minimum conditions in those years. The North-South asymmetry in the GPIR is due to a systematic hemispherical asymmetry in the NCEP atmospheric density profiles.

The Mertens et al. (2013) GPIR are about a factor of two smaller than those presented in Usoskin et al. (2010), and the altitude of the maximum in the GPIR is lower in the NAIRAS results as well. A comparison of these two computations of GCR ion rates at 90 degrees N is given in Figure 3 for both solar minimum (1965) and solar maximum (1960) conditions. The underprediction of the NAIRAS GPIR and the lower altitude of its maximum is due to the lack of pion-initiated electromagnetic cascade processes in the HZETRN version 2010 currently implemented in the NAIRAS model (Mertens et al., 2013). This deficiency will soon be rectified when the 2015 version of HZETRN is integrated into the NAIRAS model (e.g., Norman et al., 2012, 2013; Slaba et al. 2013).

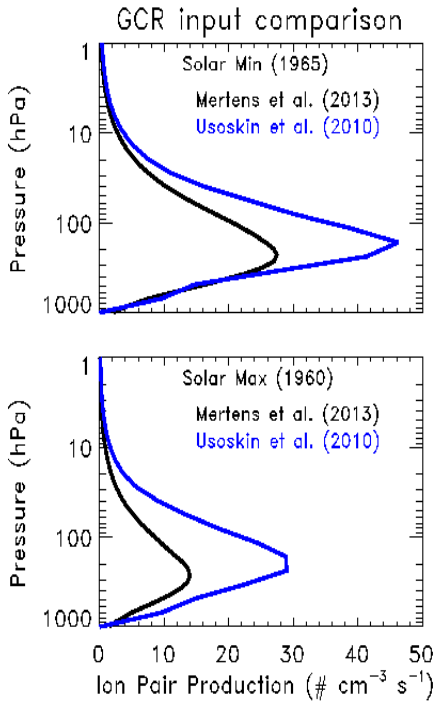

New Figure 3 caption:

NAIRAS model computed galactic cosmic ray annual average ionization rates (Mertens et al., 2013) compared to those given in Usoskin et al. (2010) for solar minimum (1965, top plot) and solar maximum (1960, bottom plot).

Authors now add several papers to the Reference list as a result of the Paper modifications:

Finlay, C. C., Maus, S., Beggan, C. D., Bondar, T. N., Chambodut, A., Chernova, T. A.,Chulliat, A., Golovkov, V. P., Hamilton, B., Hamoudi, M., Holme, R., Hulot, G., Kuang, W., Langlais, B., Lesur, V., Lowes, F. J., Lühr, H., Macmillan, S., Mandea, M., McLean, S., Manoj, C., Menvielle, M., Michaelis, I., Olsen, N., Rauberg, J., Rother, M., Sabaka, T. J., Tangborn, A.,Tøffner-Clausen, L.,Thébault, E.,Thomson, A. W. P., Wardinski, I., Wei, Z., and Zvereva, T. I., International Geomagnetic Reference Field: the eleventh generation, Geophysical Journal International, 183, 1216-1230, doi10.1111/j.1365-246X.2010.04804, 2010

Mertens, C. J., Kress, B. T., Wiltberger, M., Tobiska, W. K., Grajewski, B., and Xu, X., Atmospheric ionizing radiation from galactic and solar cosmic rays, Current Topics in Ionizing Radiation Research, Edited by Mitsuru Nenoi, InTech Publisher (ISBN 978-953-51-0196-3), 2012.

Norman, R. B., Blattnig, S. R., De Angelis, G., Badavi, F. F., and Norbury, J. W., Deterministic pion and muon tranport in Earth's atmosphere, Adv. Space Res., 50, 146-155, 2012.

Norman, R. B., Slaba, T. C., and Blattnig, S. R., An extension of HZETRN for cosmic ray initiated electromagnetic cascades, Adv. Space Res., 51, 2251-2260, 2013.

Picone, J. M., Hedin, A. E., Drob, D. P., and Aikin, A. C., NRLMSIS-00 empirical model of the atmosphere: Statistical comparisons and scientific issues, J. Geophys. Res., 107(A12), 1468, 10/1029/2002JA009430, 2002.

Slaba, T. C., Blattnig, S. R., Reddell, B., Bahadori, A., Norman, R. B., and Badavi, F. F., Pion and electromagnetic contribution to dose: Comparisons of HZETRN to Monte Carlo results and ISS data, Adv. Space Res., 52, 62-78, 2013.

Smart, D. F. and Shea, M. A., Geomagnetic cutoffs: A review for space dosimetry calculations, Adv. Space Res., 14(10), 10,787-10,796, 1994.

Smart, D. F. and Shea, M. A., A review of geomagnetic cutoff rigidities for earth-orbiting spacecraft, Adv. Space Res., 36, 2012-2020, 2005.

***Referee #1** - Accordingly, the validity of the GCR-induced cascade modelling in theNAIRAS/NZETRN model is not verified against full Montre-Carlo models and rises several questions. Unless the authors can prove that the computations of ionization are correct, the result cannot be trusted.*

Authors' Reply: See discussion above regarding these issues

Other minor comments:
***Referee #1** - 1) A brief summary is needed in the end of the abstract – are these changes important or not?*

Authors' Reply to 1): We think this issue was raised when the paper was first submitted and before it was available online. There is presently a sentence at the end of the abstract, which does indicate the importance of these atmospheric impacts. It reads "*Although these computed ozone impacts are small, GCRs provide a natural influence on ozone and need to be quantified over long time periods.*"

***Referee #1** - 2) page 33935, line 6: Please give some detail how the cutoff rigidity was calculated* from the IGRF model and please add a reference to IGRF.

Authors' Reply to 2): We now provide some information about this in the second paragraph of Section 2 of the revised paper.

Authors' modification of Paper as a result of 2): Two sentences were added to the second paragraph of Section 2 that read:

The GCR spectral flux at 1 AU travel through the magnetosphere by means of a transmission factor determined by the vertical geomagnetic cutoff rigidity computed in the International Geomagnetic Reference Field (IGRF) model (Finlay et al., 2010). The vertical cutoff rigidities are determined by numerical solutions of charged particle trajectories in the IGRF field using the techniques advanced by Smart and Shea (1994, 2005).

***Referee #1** - 3) page, line 3: "primarily protons" is not exactly correct. While protons form 90% in the particle number, heavier species constitute ~30% in the nucleon number and may contribute up to 50% in the ionization rate.*

Authors' Reply to 3): We think this issue was raised when the paper was first submitted and before it was available online. The first sentence of the Introduction had the phrase "extremely energetic charged particles (primarily protons)". As a result of the preliminary review, we removed "(primarily protons)" from that sentence.

Authors' modification of Paper as a result of 3): The first sentence of the Section 1 Introduction reads:

Galactic cosmic rays (GCRs) from outside the solar system are comprised of highly energetic charged particles and are believed to be the result of supernovae events and other high energy astrophysical processes. GCRs contain a wide range of energetic particles, which are also influenced by the Earth's magnetosphere.

>>

Reply to Referee #2

We thank Referee #2 for helpful comments and suggestions. The "Referee's Comments" are noted first and then we give our "Reply:" to the comment.

Referee 2: **Anonymous Referee #2**

Received and published: 29 December 2015

Referee #2 *General comments: The manuscript describes the atmospheric changes caused by the influence of Galactic Cosmic Rays (GCR) on the production of nitrogen and hydrogen oxides. The authors analyze the response of the chemical composition to GCR simulated with two global chemical models using several scenarios of the boundary conditions. The subject of the manuscript is relevant to the ACP scope. The paper is well written and structured. The reference list includes most of the previous publications on this subject. All figures and tables are of good quality. The results contains already known information about the influence of GCR on the chemical composition as well as some new results concerning the influence of atmospheric state (e.g., chlorine and stratospheric aerosol loading) on the global mean total column ozone response to GCR. I think the publication of the manuscript can be recommended. However, there are several issues in the manuscript (see specific) comments and some moderate revisions would be necessary before the publication.*

Specific comments:

Referee #2 *- 1. The response of the chemical composition to GCR obtained with the exploited models agrees well with the results published by Calisto et al. (2011), however it is heavily underestimated in comparison with the results of Semeniuk et al. (2011). This disagreement was briefly discussed by Mironiova et al. (2015, 10.1007/s11214-015-0185-4) and I think it should be also discussed in the paper, because it is important for the community.*

Authors' Reply to 1.: We were not aware of the review paper by Mironova et al. (2015) before, thus did not reference it in our original manuscript. The results of CMAM

given in Semeniuk et al. (2011) are discussed in Mironova et al. (2015), who note on pp. 59-60 of their paper that:

"CMAM results reveal statistically significant NO*x* increase in the entire troposphere/lower stratosphere reaching up to 100 %. The reasons for such a substantial disagreement between the simulated NO*x* responses are not clear yet. It may be explained by different background NO*x* fields in the troposphere and lower stratosphere. The absence of anthropogenic and natural NO*x* emissions together with oversimplified tropospheric chemistry in CMAM (Semeniuk et al. 2011) could lead to very small background NO*x* abundance and strong impact of the GCR induced source. This hypothesis is partially supported by closer agreement in the troposphere over the southern high latitudes, where the influence of anthropogenic and natural sources of NO*x* is the smallest.

The effectiveness of the ozone production by additional NO*x* strongly depends on the background NO*x* field. In the NO*x*-poor environment the ozone production can be very large, while for the relatively high level of NO*x* the ozone production by additional NO*x* is limited. Presumably the low background NO*x* mixing ratio in CMAM model is the reason of the large (up to 15 %) ozone enhancement in the entire troposphere, while in the CCM SOCOL significant ozone response is confined to the relatively clean southern hemisphere and reaches only 2–3 %."

It is outside the scope of this manuscript to discuss in great detail the much larger GCR-caused atmospheric changes in Semeniuk et al. (2011) compared to those given in Calisto et al. (2011) and presented here. Section 5.1 of the paper is slightly modified to note this difference in the results of previous papers.

Authors' modification of Paper as a result of 1.: We do now mention the much larger response of the CMAM model to the GCR perturbation at the end of the first paragraph in section 5.1. We add these two sentences:

As an aside, the SD-WACCM results, like those in Calisto et al. (2011), indicate a much smaller GCR-caused NOx impact than computed in Semeniuk et al. (2011). Mironova et al. (2015) propose that "the absence of anthropogenic and natural NOx emissions together with oversimplified tropospheric chemistry in CMAM" may be the reason for the larger response of the GCR perturbation in CMAM.

Add Mironova et al. (2015) to the Reference list:

Mironova, I. A., Aplin, K. L., Arnold, F., Bazilevskaya, G. A., Harrison, R. G., Krivolutsky, A. A., Nicoll, K. A., Rozanov, E. V., Turunen, E., Usoskin, I. G., Energetic Particle Influence on the Earth's Atmosphere, Space Sci. Rev., 194, 1–96, 2015

***Referee #2** - 2. Comparison of the main results against Calisto et al. (2011) and Semeniuk et al. (2011) requires some comparison of the applied ionization rates, because the difference between NAIRAS and Usoskin et al. (2010) calculations should be well characterized.*

Authors' Reply to 2.: The NAIRAS ionization rates from Mertens et al. (2013) are compared with those given in Usoskin et al. (2010) for solar minimum (1965) and solar maximum (1960) conditions in new Figure 3 in the paper now. The Mertens et al. (2013) rates are about a factor of two smaller than those given in Usoskin et al. (2010).

Authors' modification of Paper as a result of 2.: This is now discussed in the revised manuscript in the fourth paragraph of Section 2, which reads:

The Mertens et al. (2013) GPIR are about a factor of two smaller than those presented in Usoskin et al. (2010), and the altitude of the maximum in the GPIR is lower in the NAIRAS results as well, A comparison of these two computations of GCR ion rates at 90 degrees N is given in Figure 3 for both solar minimum (1965) and solar maximum (1960) conditions. The underprediction of the NAIRAS GPIR and the lower altitude of its maximum is due to the lack of pion-initiated electromagnetic cascade processes in the HZETRN version 2010 currently implemented in the NAIRAS model (Mertens et al., 2013). This deficiency will soon be rectified when the 2015 version of HZETRN is integrated into the NAIRAS model (e.g., Norman et al., 2012, 2013; Slaba et al. 2013).

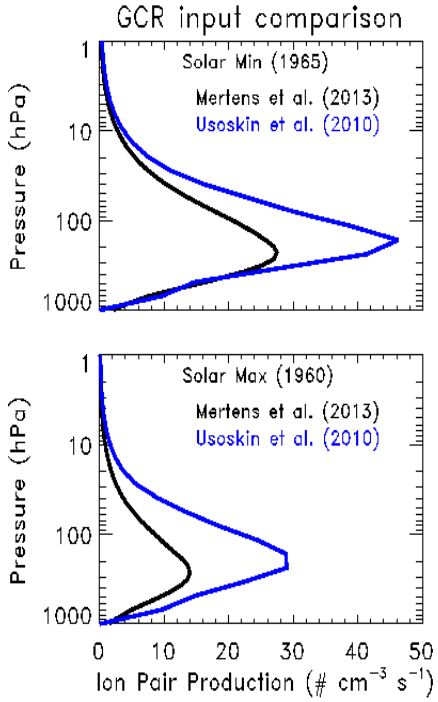

New Figure 3 caption:

NAIRAS model computed galactic cosmic ray annual average ionization rates (Mertens et al., 2013) compared to those given in Usoskin et al. (2010) for solar minimum (1965, top plot) and solar maximum (1960, bottom plot).

***Referee #2** - 3. The choice of the models is not justified. I do not understand why the models with prescribed dynamics/transport were chosen. If some influence of GCR on ozone concentration is expected than this model choice hampers the possibility to study subsequent effects of GCR on temperature, circulation and climate.*

Authors' Reply to 3.: The purpose of this paper was only to focus on the direct atmospheric composition changes caused by GCRs. The effects of GCRs on temperature and circulation had already been discussed in the Calisto et al. (2011) and

Semeniuk et al. (2011) papers. In those papers, it was clear that the GCR-caused temperature and circulation modifications also had an influence on the compositional changes. We wanted to cleanly study the GCR-caused compositional changes only, thus it was outside the scope of this paper to also study the GCR impact on temperature and circulation.

Referee #2 *- 4. Analyzing the results of sensitivity studies with their 2-D model the authors consider only global/annual mean total column ozone (GAMTCO). I think it is not a good choice because in the tropical area which contributes a lot to global mean value the influence of GCR is very small due to high cutoff rigidity. Therefore the magnitude of the GAMTCO changes caused by GCR is very small. It can be even considered negligible, because it is smaller than the measurement uncertainties. Would it be the same if the authors look at the higher latitude zones where the ionization by GCR is more pronounced.*

Authors' Reply to 4.: We computed the GCR impact on the annual average global total ozone (AAGTO) because GCRs impact the atmosphere at all latitudes. We agree that the largest impact of the GCRs is at the highest latitudes. We have computed the GCR impact at polar latitudes only (60-90 degrees South and 60-90 degrees North) and present them in the new Figure 9. There are many similarities in shape between the annual average polar total ozone (AAPTO) and the AAGTO, however, the AAPTO is always larger. For example, from the bottom plots of Figure 8 (old Figure 7) and new Figure 9: In 1960 the AAGTO is computed to be -0.13% while the AAPTO is computed to be -0.18%. In 2010 the AAGTO is computed to be -0.11% while the AAPTO is computed to be -0.27%. Thus, the polar differences tend to be larger by the end than they were at the start of the simulation period.

Authors' modification of Paper as a result of 4.: This is now discussed in Section 5.2 in the new fourth paragraph, which reads:

The GCR-caused atmospheric changes are larger at higher latitudes, thus we also compute the annual average polar total ozone (AAPTO). The AAPTO is calculated using the model output only at polar latitudes (60-90 degrees South and 60-90 degrees North) and is given in Figure 9. Both the AAGTO (Figure 8) and the AAPTO (Figure 9) have similar shapes for the total ozone change in the two regions plotted (1000 to 100 hPa and 100 to 1 hPa). In 1960 the AAGTO for the entire troposphere and stratosphere (1000 to 1 hPa) is computed to be -0.13% (see Figure 8, bottom) while the AAPTO is computed to be -0.18% (see Figure 9, bottom). In 2010 the AAGTO for the troposphere and stratosphere is computed to be -0.11% (see Figure 8, bottom) while the AAPTO is computed to be -0.27% (see Figure 9, bottom). Thus, the polar differences tend to be larger by the end than they were at the start of the simulation period.

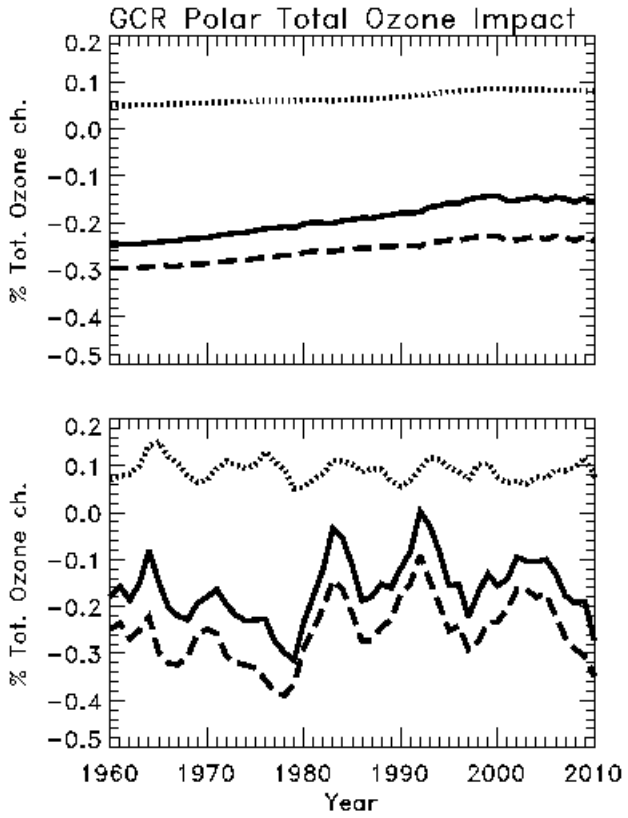

New Figure 9 caption:

GSFC 2-D model GCR-computed impacts of annual average polar total ozone (AAPTO) between 1000 and 100 hPa (dotted black), between 100 and 1 hPa (dashed black), and for the entire troposphere and stratosphere, 1000 to 1 hPa, (solid black) over the 1960-2010 time period. The top plot shows the comparison of simulation A1_GCR_GSFC to A_Base_GSFC. The bottom plot shows the comparison of simulation E_GCR_GSFC to E_Base_GSFC.

***Referee #2** Minor/technical issues:*

***Referee #2** - 1. page 33935, line 26: It reads like GCR produce constituents w/o ionization. I suggest reformulate, because NOx, HOx production is the results of ionization.*

Authors' Reply to 1.: The GCRs can produce NOx without ionization. Charged particles can directly dissociate molecular nitrogen (N2) into nitrogen atoms. For example, the N atoms, especially in excited states N(2D) or N(2P), can react quickly with molecular oxygen (O2) to form NO + O. N+ atoms can also lead to production of NO+. These processes are discussed in G. Brasseur and S. Solomon, Aeronomy of the Middle Atmosphere, D. Reidel Publishing Company, 1995, especially see Chapter 6. A more detailed discussion of the dissociation of N2 and O2 by very energetic protons and the associated secondary electrons is given in H. S. Porter. C. H. Jackman, and A. E. S.

Green, Efficiencies for production of atomic nitrogen and oxygen by relativistic proton impact in air, The Journal of Chemical Physics, 65, 154-167, (1976).

It is true that HOx production requires complex chemistry involving positive ions. This is explained in Section 3.

Since NOx can be produced through direct dissociation of N2 (and without ionization), we have not changed the Section 3 title.

Referee #2 *- 2. page 33937, lines 5-19: Are lightning and aircraft emissions included in WACCM?*
The authors said they are included in 2-D GSFC.

Authors' Reply to 2.: Yes, lightning and aircraft emissions are included in WACCM (see section 3.4 of Lamarque et al.,The CAM-chem: description and evaluation of interactive atmospheric chemistry in the Community Earth System Model, Geosci. Model Dev., 5, 369–411, 2012). This is now noted in Section 4.1.

Authors' modification of Paper as a result of 2.: This is now discussed in the revised manuscript at the end of the second paragraph of Section 4.1, which reads:

Tropospheric NOx production from lightning and aircraft is included as described in Lamarque et al. (2012).

Add Lamarque et al. (2015) to the Reference list:

Lamarque, J.-F., Emmons, L. K., Hess, P. G., Kinnison, D. E., Tilmes, S., Vitt, F., Heald, C. L., Holland, E. A., Lauritzen, P. H., Neu, J., Orlando, J. J., Rasch, P. J., and Tyndall, G. K.,The CAM-chem: description and evaluation of interactive atmospheric chemistry in the Community Earth System Model, Geosci. Model Dev., 5, 369–411, doi:10.5194/gmd-5-369-2012, 2012.

Referee #2 *- 3. Section 4.2: How good is representation of tropospheric chemistry in 2-D environment? The chemistry is non linear, but it is necessary to use zonal mean fields. It would be interesting to compare OH distribution from the two applied models.*

Authors' Reply to 3.: The speed of the 2-D model makes it a valuable tool in this study, which includes a number of multi-decadal simulations. We agree that a 2-D model may not represent tropospheric chemistry as well as a 3-D model. However, the GSFC 2-D model's troposphere has been improved recently as was described in section 4.2 (pp. 33938-33939). Since the reviewer specifically asks about OH, we also note that for the current paper, the model tropospheric OH is specified from the monthly varying OH field documented in Spivakovsky et al. (2000). The GSFC 2-D model recently participated in a SPARC Project investigating the "Lifetimes of Stratospheric Ozone-Depleting Substances, Their Replacements, and Related Species" edited by M.K. W. Ko et al. and published in December 2013 (SPARC Report No. 6, WCRP-15/2013). This report is available online at http://www.sparc-climate.org/publications/sparc-reports/sparc-report-no6/. A profile of OH values is given in Figures 5.10 and 5.11 of that report and shows the GSFC 2-D model with reasonable agreement to the five different three-dimensional models with chemistry.

The annual average OH distributions for year 2009 from WACCM and the GSFC 2-D model are given below. Both models show larger tropospheric amounts in the tropics (~0.05 to 0.2 pptv) and lesser amounts at higher latitudes (~0.005 to 0.1 pptv). Generally, the two models' tropospheric OH abundances are within 30% of each other, although the GSFC 2-D models' upper tropospheric OH amounts can be up to 50% less than WACCM values for mid to high latitudes.

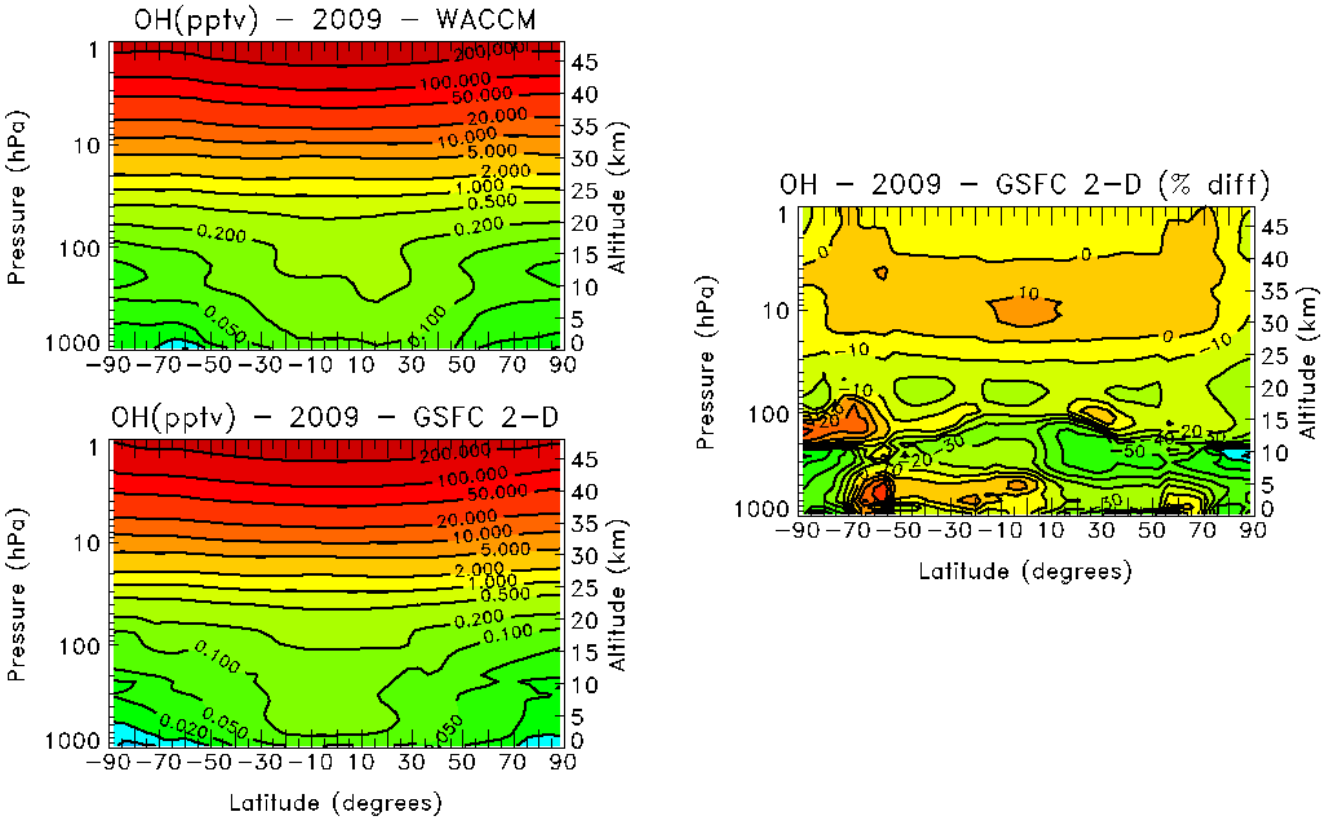

Figure on Comparison of Models' OH.

Annual average OH distributions for year 2009 from WACCM (top left) and the GSFC 2-D model (bottom left) are shown. Percentage difference of the GSFC 2-D model OH from WACCM OH (right) is also shown.

Authors' modification of Paper as a result of 3.: A sentence (third) has been added in paragraph 4 of Section 4.2, which reads:

The model tropospheric OH is specified from the monthly varying OH field documented in Spivakovsky et al. (2000).

Add Spivakovsky et al. (2000) to the Reference list:

Spivakovsky, C. M., Logan, J. A., Montzka, S. A., Balkanski, Y. J., Foreman-Fowler, M., Jones, D. B. A., Horowitz, L. W., Fusco, A. C., Brenninkmeijer, C. A. M., Prather, M. J., Wofsy, S. C., and McElroy, M. B., Three-dimensional climatological distribution of tropospheric OH: Update and evaluation, J. Geophys. Res., 105, 8931-8980, doi:10.1029/1999JD901006, 2000.

Referee #2 *- 4. page 33940, lines 22-23: Not proper explanation. I think NMHC and VOC's included in the both models also play important role.*

Authors' Reply to 4.: NMHC and VOC's are specified in the GSFC 2-D model using output from a three-dimensional model (the Global Modeling Initiative's (GMI) combined stratosphere-troposphere chemistry and transport model), see the fourth paragraph of Section 4.2. A four-year average (2004-2007), which changes seasonally but repeats yearly, of the GMI model's output is used. Thus the annual average values of NMHC and VOC's do not increase over the 1960-2010 time period.

We do, however, agree with the referee that our explanation is not totally accurate. We have analyzed this issue by completing several sensitivity studies with the GSFC 2-D model using different temporally changing levels of CH4. We have found that the CH4 increase is only responsible for about one-third of the "tropospheric" ozone increase over the period 1960-2010. In the process of investigating this issue, we realized that the "tropospheric column" line was mislabeled in Figure 7. This line represents ozone at pressures greater than 100 hPa, which is the troposphere in the tropics, but overestimates the tropospheric extent at higher latitudes. We have redone some of the discussion in Section 5.2 to correct this.

Besides CH4, we found that the increase in chlorine levels over this time period also led to an increase in column ozone between 1000 and 100 hPa. Chlorine thus becomes more important in the control of ozone over the 1960-2010 time period. This means that the formation of ClONO2 through the reaction ClO+NO2+M → ClONO2+M becomes more influential when GCRs produce NOx. Thus, the GCRs become more important in affecting ozone variation in the lowest part of the stratosphere (at pressures greater than 100 hPa) at higher latitudes over those 51 years.

Authors' modification of Paper as a result of 4.: The second sentence of the fourth paragraph of Section 4.2 is modified to read:

For this, the following quantities are specified using a four-year average (2004-2007) output from recent simulations of the Global Modeling Initiative's (GMI) combined stratosphere-troposphere chemistry and transport model…

The third sentence of the second paragraph in Section 5.1 is modified to read:

The GCR-caused ozone increase is due to two processes: 1) the GCR-produced NO reacts with CH4 oxidation products (see, also Krivolutsky et al., 2001); and 2) the GCR-produced NO2 reacts with ClO to form ClONO2 and reduces the chlorine-caused ozone loss.

The first three paragraphs of Section 5.2 are also modified (because of the mislabeling problem noted above) to read:

The GSFC 2-D model gives fairly similar results to SD-WACCM (compare Figs. 4 and 5) and is significantly faster computationally to use for longer-term simulations. Thus, the GSFC 2-D model was used in several sensitivity study simulations described in Table 1 (and Sect. 4.2) to investigate the longer term GCR-caused changes, particularly focusing on annual average global total ozone (AAGTO) as well as global column ozone in the two regions between 1000 and 100 hPa and between 100 and 1 hPa. The GCR-caused change in ozone in those two regions, separately, and for the entire troposphere and stratosphere (1000 to 1 hPa) is computed for two pairs of scenarios: (1) Fig. 8 (top) shows a comparison of the first pair (A1_GCR_GSFC to

A_Base_GSFC), which are simplified representations of the atmosphere with a climatological mean transport (changes daily, but repeats yearly) in both scenarios and a mean GCR input (constant throughout the simulation) in A1_GCR_GSFC; and (2) Fig. 8 (bottom) shows a comparison of the most comprehensive pair (E_GCR_GSFC to E_Base_GSFC), which include interannually varying transport, sulfate aerosol surface area, and solar cycle photon flux variation in both scenarios and an interannually varying GCR input in E_GCR_GSFC.

First, focus on the results intercomparing scenarios A1_GCR_GSFC to A_Base_GSFC (see Fig. 8, top): the GCR-caused column ozone between 1000 and 100 hPa showed an increase from +0.03% up to ~+0.05% over the 1960–2010 time period, driven partly by increases in CH4 over those 51 years. The GCR-caused column ozone between 100 and 1 hPa also showed a time dependent increase, but started in year 1960 at -0.19% ending up at -0.12% in year 2010. The GCR-caused total AAGTO follows the increases in the two regions noted above, starting at -0.16% in year 1960 and increasing to ~-0.07% in year 2010.

Second, intercompare the more complete simulations E_GCR_GSFC to E_Base_GSFC (see Fig. 8, bottom): the GCR-caused column ozone changes between 1000 and 100 hPa showed a significant variation from ~+0.03% to ~+0.07% over the 1960–2010 time period. The GCR-caused column ozone changes between 100 and 1 hPa also showed substantial variation giving -0.23% in 1979 and -0.02% in 1992. The GCR-caused total AAGTO followed these variations, with a low of -0.19% in 1979 and a high of +0.03% in 1992.

Figure 8 (old Figure 7) caption has been modified (because of the mislabeling problem noted above) to read:

Figure 8. *GSFC 2-D model GCR-computed impacts of annual average global total ozone (AAGTO) between 1000 and 100 hPa (dotted black), between 100 and 1 hPa (dashed black), and for the entire troposphere and stratosphere, 1000 to 1 hPa, (solid black) over the 1960–2010 time period. The top plot shows the comparison of simulation A1_GCR_GSFC to A_Base_GSFC. The bottom plot shows the comparison of simulation E_GCR_GSFC to E_Base_GSFC.*

Referee #2 *- 5. page 33943, second paragraph: In Figure 7(upper panel) the increase of tropospheric ozone is explained by CH4 increase. Why it is not the case for Figure 7 (lower panel). It would be interesting to explain.*

Authors' Reply to 5.: We have tried to investigate this model predicted variation of "tropospheric" ozone from one year to the next. As indicated above, we plotted ozone between 1000 and 100 hPa with the dashed line rather than "only" tropospheric ozone. Thus, variations in the lowest stratospheric amounts of ozone also have an impact on this variation. As discussed in the paper, the background total chlorine, aerosol surface area, and solar cycle variation of the GCR impact can also have a large influence on the ozone variations. For example, the increase in ozone between 1000 and 100 hPa from 1960 to 1965 is mainly influenced by the increase in GCR NOx production during solar minimum of the mid-1960s and the increase in aerosol surface area in 1963-64. These two processes increase ozone through the following: 1) The

GCR NOx production leads to a tropospheric ozone increase primarily through reaction with CH4 (as explained in Krivolutsky et al. 2001); and 2) the increase in aerosol surface area leads to a decrease in stratospheric ozone loss due to the NOx catalytic cycle, thus any increase in NOx (such as through GCRs) would cause less ozone destruction.

Referee #2 *- 6. page 33945, line 21: I think "intensity" should be added after "reactions"*

Authors' Reply to 6.: The word "intensity" has now been added after "reactions".

Authors' modification of Paper as a result of 6.: The third sentence in section 5.2.2 has been modified to read:

Enhanced aerosol surface area results in an increase in heterogeneous reactions' intensity on the sulfate aerosols.

Atmospheric changes caused by galactic cosmic rays over the period 1960-2010

Charles H. Jackman[1], Daniel R. Marsh[2], Douglas E. Kinnison[2], Christopher J. Mertens[3], and Eric L. Fleming[4,5]

[1](Emeritus, NASA Goddard Space Flight Center, Greenbelt, MD, U.S.A.)

[2](National Center for Atmospheric Research, Boulder, CO, U.S.A.)

[3](NASA Langley Research Center, Hampton, VA, U.S.A.)

[4](NASA Goddard Space Flight Center, Greenbelt, MD, U.S.A.)

[5](Also at Science Systems and Applications, Inc., Lanham, MD, U.S.A.)

Correspondence to: Charles H. Jackman (Charles.H.Jackman@nasa.gov)

Abstract

The Specified Dynamics version of the Whole Atmosphere Community Climate Model (SD-WACCM) and the Goddard Space Flight Center two-dimensional (GSFC 2-D) models are used to investigate the effect of galactic cosmic rays (GCRs) on the atmosphere over the 1960-2010 time period. The Nowcast of Atmospheric Ionizing Radiation for Aviation Safety (NAIRAS) computation of the GCR-caused ionization rates are used in these simulations. GCR-caused maximum NO_x increases of 4-15% are computed in the Southern polar troposphere with associated ozone increases of 1-2%. NO_x increases of ~1-6% are calculated for the lower stratosphere with associated ozone decreases of 0.2-1%. The primary impact of GCRs on ozone was due to their production of NO_x. The impact of GCRs varies with the atmospheric chlorine loading, sulfate aerosol loading, and solar cycle variation. Because of the interference between the NO_x and ClO_x ozone loss cycles (e.g., the $ClO + NO_2 + M \rightarrow ClONO_2 + M$ reaction) and the change in the importance of ClO_x in the ozone budget, GCRs cause larger atmospheric impacts with less chlorine loading. GCRs also cause larger atmospheric impacts with less sulfate aerosol loading and for years closer to solar minimum. GCR-caused decreases of annual average global total ozone (AAGTO) were computed to be 0.2% or less with GCR-caused tropospheric column ozone increases of 0.08% or less and GCR-caused stratospheric column ozone decreases of 0.23% or less. Although these computed ozone impacts are small, GCRs provide a natural influence on ozone and need to be quantified over long time periods.

1 Introduction

Galactic cosmic rays (GCRs) from outside the solar system are comprised of highly energetic charged particles and are believed to be the result of supernovae events and other high energy astrophysical processes. GCRs contain a wide range of energetic particles, which are also influenced by the Earth's magnetosphere. High energy GCRs not only penetrate further into the atmosphere, but can also cause atmospheric effects outside the polar cap regions. The flux of GCRs is larger during solar minimum, when the reduced solar magnetic field less effectively shields the solar system from the particles.

The influence of galactic cosmic rays (GCRs) on the middle atmosphere has been studied since the 1970's (e.g., Warneck 1972; Ruderman and Chamberlain, 1975; Nicolet 1975; Jackman et al., 1980, 1987, 1996; Thorne 1980; Garcia et al., 1984; Legrand et al., 1989; Jackman 1991, 1993; Müller and Crutzen, 1993; Vitt and Jackman, 1996; Krivolutsky et al., 1999, 2001, 2002; Vitt et al., 2000; Semeniuk et al., 2011; Calisto et al., 2011). These previous studies made use of GCR-produced ionization rates (GPIR) in computing atmospheric chemistry impacts. The GPIR were deduced primarily in a couple of different methodologies.

For example, Nicolet (1975) made use of balloon soundings and ionization chambers to compute the GPIR. Several of the other earlier studies roughly followed the Nicolet (1975) methodology for inclusion of GPIR in atmospheric analyses. A more recent study by Calisto et al. (2011) primarily relied on the computations of the Cosmic Ray induced Cascade: Application for Cosmic Ray Induced Ionization (CRAC:CRII) of Usoskin et al. (2010) to deduce the GPIR. Another method of computing GPIR has been developed by the Nowcast of Atmospheric Ionizing Radiation for Aviation Safety (NAIRAS) team at NASA Langley Research Center (see Mertens et al., 2013). The NAIRAS-deduced GPIR has been computed over the years 1960-2010. The solar cycle shows substantial variation over this 51-year time period, which is reflected in the GPIR.

GCRs also affect the atmosphere through the production of the important constituent families of NO_x (N, NO, NO_2) and HO_x (H, OH, HO_2) either directly or through a photochemical sequence. The NAIRAS-deduced GPIR and subsequent NO_x and HO_x production can be used in atmospheric models to predict impact on constituents over the 1960-2010 period. We use two models, the Specified Dynamics – Whole Atmosphere Community Climate Model (SD-WACCM) and the Goddard Space Flight Center (GSFC) two-dimensional (2-D) model, to

study the influence of GCRs on the atmosphere over these 51 years. SD-WACCM is used for detailed studies of the impact of GCRs on minor atmospheric constituents. The GSFC 2-D model helps in the quantification of the changing GCR influence between 1960 and 2010 as the chlorine-loading, sulfate aerosol amount, solar cycle, and dynamics vary over this time period. The fast computational speed of the GSFC 2-D model (compared with SD-WACCM) allows a number of simulations to investigate the sensitivity of the GCR influence in different changing background atmospheres.

This paper is divided into six primary sections, including the Introduction. The NAIRAS GCR ionization rate computation is discussed in Section 2 and the GCR-induced production of HO_x and NO_x are discussed in Section 3. A description of the two models (SD-WACCM and GSFC 2-D) used in this work are given in Section 4. Model results (both SD-WACCM and GSFC 2-D) for several GCR-caused atmospheric constituent changes are shown in Section 5. The conclusions are presented in Section 6.

2 NAIRAS GCR ionization rate

The Nowcast of Atmospheric Ionizing Radiation for Aviation Safety (NAIRAS) team at NASA Langley Research Center (see http://sol.spacenvironment.net/ ~nairas/) has developed and integrated a model to include GCRs into their ionizing radiation computation. The interplanetary magnetic field varies over a solar cycle and provides a modulation of the GCR spectral flux, which has been referred to as a solar modulation potential (e.g., Badhwar and O'Neill, 1996). For real-time application of the NAIRAS model, ~~F~~four real-time, high-latitude, ground-based neutron monitor count rate measurements are used to cross correlate with the solar modulation potential and provide the NAIRAS model's GCR spectral flux incident on the Earth for penetration into and through the atmosphere. NAIRAS is a physics-based model that maximizes the use of measurement input data (Mertens et al., 2013, and references therein).

In the NAIRAS model, GCRs travel from outside the heliosphere to 1 AU by the Badhwar and O'Neill (1992, 1994, 1996) and O'Neill (2010) NASA model, with the solar modulation potential determined from measurements of ground-based neutron monitor count rates. The GCR spectral flux at 1 AU travel through the magnetosphere by means of a transmission factor determined by the vertical geomagnetic cutoff rigidity computed in the International Geomagnetic Reference Field model (Finlay et al., 2010). The vertical cutoff rigidities are determined by numerical solutions of charged particle trajectories in the IGRF field using the

Formatted: Font: (Default) Times New Roman, Not Italic

Formatted: Font: (Default) Times New Roman, Not Italic

techniques advanced by Smart and Shea (1994, 2005).After transmission through the magnetosphere, the GCR spectral flux travels through the neutral atmosphere using the NASA HZETRN deterministic transport code (Mertens et al., 2012). The global distribution of atmospheric mass density is obtained from NCAR/NCEP Reanalysis 1 data at pressure levels larger than 10 hPa (Kalnay et al., 1996) and the Naval Research Laboratory Mass Spectrometer and Incoherent Scatter model atmosphere data at pressure levels less than 10 hPa (Picone et al., 2002).

The NAIRAS model has been used to compute the annual average GCR-produced ionization rates (GPIR) for the 1960-2010 time periods~~. These ionization rates have been verified by comparing with balloon ion chamber measurements taken by Neher (1967) and also with ionization rates with Geant4 Monte Carlo transport code results reported recently by Calogovic et al. (2010) and Gronoff et al. (2015).~~ For these time periods, measurements from the Thule and Izmiran neutron monitor stations were used to determine the solar modulation potential. GPIR in the NAIRAS model are computed by multiplying the dose rate in air by the atmospheric density, divided by 35 eV per ion-pair. The annual average GPIR from the NAIRAS model for two years, 2002 and 2009, are presented in Figure 1. This shows the inverse relationship between GPIR and solar activity. Year 2002 is very close to solar maximum and shows a smaller GPIR with maximum ionization rates of nearly 15 cm^{-3} s^{-1}, whereas year 2009 is very close to solar minimum with about a factor of two larger maximum ionization rate of 30 cm^{-3} s^{-1}. The time-dependent variation in the GPIR at 90°S and 90°N is given in Figure 2. Peaks in GPIR occur in 1965, 1977, 1987, 1997, and 2009, reflective of solar minimum conditions in those years. The North-South asymmetry in the GPIR is due to a systematic hemispherical asymmetry in the NCEP atmospheric density profiles.

The Mertens et al. (2013) GPIR are about a factor of two smaller than those presented in Usoskin et al. (2010), and the altitude of the maximum in the GPIR is lower in the NAIRAS results as well. A comparison of these two computations of GCR ion rates at 90 degrees N is given in Figure 3 for both solar minimum (1965) and solar maximum (1960) conditions. The underprediction of the NAIRAS GPIR and the lower altitude of its maximum is due to the lack of pion-initiated electromagnetic cascade processes in the HZETRN version 2010 currently implemented in the NAIRAS model (Mertens et al., 2013). This deficiency will soon be rectified when the 2015 version of HZETRN is integrated into the NAIRAS model (e.g., Norman et al., 2012, 2013; Slaba et al. 2013).

Formatted: Font: (Default) Times New Roman, Not Italic

Formatted: Font: (Default) Times New Roman, Not Italic

Formatted: Font: (Default) Times New Roman, Not Italic

Formatted: Left, Line spacing: 1.5 lines

3 NO_x (N, NO, NO_2) and HO_x (H, OH, HO_2) production

Besides ionization, GCRs also produce the important constituent families of NO_x (N, NO, NO_2) and HO_x (H, OH, HO_2) either directly or through a photochemical sequence. NO_x is produced when the cosmic rays (primarily protons and their associated secondary electrons) dissociate N_2 as they precipitate into the atmosphere. Here it is assumed that 1.25 N atoms are produced per ion pair and the proton impact of N atom production is divided between the ground state N(^{4}S) (45% or 0.55 per ion pair) and excited state N(^{2}D) (55% or 0.7 per ion pair) nitrogen atoms (Porter et al., 1976). GCRs also result in the production of HO_x through complex positive ion chemistry (Solomon et al., 1981). The charged particle-produced HO_x is a function of ion pair production and altitude and is included in model simulations using a lookup table from Jackman et al. (2005, Table 1), which is based on the work of Solomon et al. (1981). Each ion pair results in the production of about two HO_x constituents for the troposphere, stratosphere, and lower mesosphere and less than two HO_x constituents for the middle and upper mesosphere.

4 Model Predictions

4.1 Description of the Specified Dynamics – Whole Atmosphere Community Climate Model

The latest version of the NCAR Community Earth System Model, version 1 (CESM1) Specified Dynamics – Whole Atmosphere Community Climate Model (SD-WACCM) was used to predict the impact of GCRs on the atmosphere. SD-WACCM is a global model with 88 vertical levels from the surface to 4.5×10^{-6} hPa (approximately 140 km geometric height). SD-WACCM was most recently described in Wegner et al. (2013) and Solomon et al. (2015) and uses prescribed dynamical fields (e.g., see Lamarque et al., 2012) from the NASA Global Modeling and Assimilation Office Modern-Era Retrospective Analysis for Research and Applications (MERRA) (Rienecker et al., 2011). Temperature, zonal and meridional winds, and surface pressure are used to drive the physical parameterizations that control boundary layer exchanges, advective and convective transport, and the hydrological cycle. The SD-WACCM meteorological fields are relaxed toward the MERRA reanalysis fields using the approach described in Kunz et al. (2011).

The chemical module of SD-WACCM is based upon the 3-D chemical transport Model of Ozone and Related Tracers, Version 3 (MOZART) (Kinnison et al., 2007). It includes a

detailed representation of the chemical and physical processes from the troposphere through the lower thermosphere. The species included within this mechanism are contained within the O_x, NO_x, HO_x, ClO_x, and BrO_x chemical families, along with CH_4 and its degradation products. SD-WACCM also includes 17 primary nonmethane hydrocarbons and related oxygenated organic compounds (Emmons et al., 2010). This mechanism contains 134 species, 420 chemical reactions, with 17 heterogeneous reactions on multiple aerosol types (i.e., sulfate, nitric acid trihydrate, and water-ice; Solomon et al., 2015). Reaction rates have been updated to JPL-2010 (Sander et al., 2011). Tropospheric NO_x production from lightning and aircraft is included as described in Lamarque et al. (2012).

For this work, the SPARC Chemistry Climate Model Initiative (CCMI), REFC1 scenario was used (see Eyring et al., 2013). This scenario included observed time-dependent evolution of: greenhouse gases (GHGs); ozone depleting substances (ODSs); sea surface temperatures and sea ice concentrations (SSTs/SICs); stratospheric sulfate surface area densities (SADs); and 11-year solar cycle variability, which includes spectrally resolved solar irradiances.

Formatted: Font: (Default) Times New Roman, Not Italic

Formatted: Font: (Default) Times New Roman, Not Italic, Subscript

Formatted: Font: (Default) Times New Roman, Not Italic

4.2 Description of the Goddard Space Flight Center Two-Dimensional Model

The most recent version of the Goddard Space Flight Center (GSFC) two-dimensional (2-D) atmospheric model was used to predict the impact of GCRs on the atmosphere. This model was first discussed over 25 years ago (Douglass et al. 1989; Jackman et al. 1990) and has undergone extensive improvements over the years (e.g., Considine et al. 1994; Jackman et al. 1996; Fleming et al. 1999, 2007, 2011, 2015). The vertical range of the model, equally spaced in log pressure, is from the ground to approximately 92 km (0.0024 hPa) with about a 1 km grid spacing. The model has a 4^o latitude grid spacing.

The specified transport version of the model is used for this study. Here, the model transport fields are derived using daily average global winds and temperatures from the National Centers for Environmental Prediction-National Center for Atmospheric Research (NCEP-NCAR) reanalysis project for years 1960-1978 (Kalnay et al. , 1996; Kistler et al. , 2001)) and the MERRA meteorological analyses for years 1979-2010. Thirty-day running averages of the residual circulation, eddy diffusion, zonal mean wind, and zonal mean temperature are computed using the methodology detailed in Fleming et al. (2007). For use in some of the simulations a climatological average was constructed of the transport over these years and

applied it over the simulated periods. The averaged transport fields change daily, but repeat yearly.

The ground boundary conditions in the GSFC 2-D model for the ozone depleting substances are taken from WMO (2014) for years 1960-2010. The model uses a chemical solver described in Jackman et al. (2005) and Fleming et al. (2007, 2011). For these computations, the photochemical gas and heterogeneous reaction rates and photolysis cross sections have been updated to the Jet Propulsion Laboratory recommendations (Sander et al., 2011) with further updates based on SPARC ~~Ko et al.~~ (2013).

The model tropospheric chemistry scheme has also been updated to include the following species: CH_3OH, C_2H_6, CH_3CHO, CH_3CO_3, $CH_3C(O)OOH$, $CH_3CO_3NO_2$ (peroxy acetyl nitrate, PAN), $C_2H_5O_2$, C_2H_5OOH, CH_3COCH_3 (acetone), and C_5H_8 (isoprene). For this, the following quantities are specified using a four-year average (2004-2007) of output from recent simulations of the Global Modeling Initiative's (GMI) combined stratosphere-troposphere chemistry and transport model (Strahan et al., 2007; Duncan et al., 2007; Strode et al. 2015): surface emissions of CH_2O, CO, NO_x,C_2H_6, and isoprene; surface mixing ratio boundary conditions for acetone, and tropospheric NO_x production from lightning and aircraft. The model tropospheric OH is specified from the monthly varying OH field documented in Spivakovsky et al. (2000). Surface dry deposition rates for H_2O_2, CH_2O, CH_3OOH, HNO_3, NO_2, N_2O_5, PAN, and O_3, and tropospheric washout rates for HO_2, H_2O_2, CH_2O, CH_3OOH, HONO, HNO_3, HO_2NO_2, NO_2, NO_3, and N_2O_5 are also specified from the GMI output. The resulting 2-D distributions of tropospheric NO_x and ozone (as well as HNO_3, CO, C_2H_6, and PAN) compare well with the GMI simulations and the ozone climatology compiled by McPeters et al. (2007). This allows the model to be used to simulate the GCR perturbations in the stratosphere and troposphere addressed in this study.

Formatted: Normal, Space Before: 0 pt, Line spacing: single, Don't adjust space between Latin and Asian text, Don't adjust space between Asian text and numbers

Formatted: Font: (Default) Times New Roman, Not Italic

Formatted: Font: (Default) Times New Roman, Not Italic

4.3 Model simulations

We conducted fourteen model simulations with the two models, which are all briefly described in Table 1. SD-WACCM was used for two simulations, both over the period 2000-2010. One of the SD-WACCM simulations did not include GCRs (simulation *Base_SD-W*), whereas the other did (simulation *GCR_SD-W*).

The GSFC 2-D model was used for twelve simulations, all over the 51-year period 1960-2010. The transport was specified for all simulations, either interannually varying with

NCEP-NCAR data for years 1960-1978 and with MERRA data for years 1979-2010 or with a climatological average of those data over the 1960-2010 time period. Five of the simulations (labeled **_Base_GSFC*) did not include GCRs and seven of the simulations (labeled **_GCR_GSFC*) did include GCRs. Four simulations (*A1_GCR_GSFC, B1_GCR_GSFC, C_GCR_GSFC, and D_GCR_GSFC*) used a 51-year average of the GCR amount and three simulations (*A2_GCR_GSFC, B2_GCR_GSFC, and E_GCR_GSFC*) included the interannual variation of GCRs. These simulations investigated the impact of GCRs in a changing atmosphere of different chlorine-loading, sulfate aerosol amount, solar photon flux, and dynamics over this time period.

5 Results

SD-WACCM and GSFC 2-D model simulations were compared to delineate the GCR-caused changes under different atmospheric conditions. Model simulations were compared for the year 2009 (solar minimum, GCR maximum) to determine the GCR impact on several constituents in section 5.1. The influence of GCRs over the solar cycle is also shown in section 5.1 (comparing year 2009 to year 2002). Changing atmospheric conditions over the years 1960-2010 and their impact on the GCR atmospheric influence are shown in section 5.2. In particular, GCR-caused global total ozone changes in the different regions of the atmosphere (troposphere, stratosphere, and total) are discussed in section 5.2 as well as the global total ozone changes caused by GCRs with different imposed atmospheric conditions. Finally, the GCR-caused NO_y production is given in comparison to the N_2O oxidation-caused NO_y production in section 5.3.

5.1 NO_x, Ozone, HO_x, and HNO_3

The GCR-caused NO_x ($NO+NO_2$) impact is shown in Figure 43 (top) for SD-WACCM and in Figure 54 (top) for the GSFC 2-D model. NO_x is mostly enhanced throughout the domain from 1000-1 hPa with largest increases (>15%) in the south polar troposphere. GCR-caused NO_x increases over 6% are computed in the north polar lower stratosphere. Although there are differences between the SD-WACCM and GSFC 2-D model computations shown here and those computed by Calisto et al. (2011), there are many similarities including the larger computed GCR-caused NO_x impact in the south polar tropospheric region compared with the north polar tropospheric region. The larger percentage change in the SH polar (60-90°S) troposphere is due to this region being significantly cleaner (NO_x background levels of 5-20 pptv) compared to north polar (60-90°N) troposphere (background levels of 20-50 pptv). As

Formatted: Font: (Default) Times New Roman, Not Italic

an aside, the SD-WACCM results, like those in Calisto et al. (2011), indicate a much smaller GCR-caused NOx impact than computed in Semeniuk et al. (2011). Mironova et al. (2015) propose that "the absence of anthropogenic and natural NO_x emissions together with oversimplified tropospheric chemistry in CMAM" may be the reason for the larger response of the GCR perturbation in CMAM.

The GCR-caused ozone impact is shown in Figure 43 (bottom) for SD-WACCM and in Figure 54 (bottom) for the GSFC 2-D model. Ozone is mostly enhanced in the troposphere and lowest part of the stratosphere with largest increases of 1-2% from GCRs in the south polar troposphere in 2009. The GCR-caused ozone increase is due to two processes: 1) the NO reacting with CH_4 oxidation products (see, also Krivolutsky et al., 2001):

For example, $CH_4 + OH \rightarrow CH_3 + H_2O$
$CH_3 + O_2 + M \rightarrow CH_3O_2 + M$
$CH_3O_2 + NO \rightarrow CH_3O + NO_2$
$NO_2 + h\nu \rightarrow NO + O$
$O + O_2 + M \rightarrow O_3 + M$

and 2) the GCR-produced NO_x reacts with ClO to form $ClONO_2$ and reduces the chlorine-caused ozone loss.

Ozone is decreased in most of the stratosphere due to the NO_x catalytic ozone depletion cycle:

$NO + O_3 \rightarrow NO_2 + O_2$
$NO_2 + O \rightarrow NO + O_2$
Net: $O_3 + O \rightarrow O_2 + O_2$

GCR-caused NO_x increases of ~1-6% are calculated for the lower stratosphere and cause ozone decreases of 0.2-1%. Our computed ozone impacts are similar to those previously discussed in Krivolutsky et al. (2001) and Calisto et al. (2011).

The computed impact of GCRs on HO_x and HNO_3 using SD-WACCM is given in Figure 65. Although GCRs produce HO_x (see section 3), HO_x decreases are computed throughout most of the atmosphere (Figure 65, top). This is caused by the NO_x increases which remove OH via the reaction

$OH + NO_2 + M \rightarrow HNO_3 + M,$

leading to HNO_3 enhancements (Figure 65, bottom). Again, these results are similar to those discussed in Calisto et al. (2011).

The SD-WACCM computations can also be used to address the question of the change in GCR influence over a solar cycle. The focus in this section has been on year 2009 since that

Formatted: Font: (Default) Times New Roman, Not Italic, Subscript
Formatted: Font: (Default) Times New Roman, Not Italic
Formatted: Font: (Default) Times New Roman, Not Italic
Formatted: Font: (Default) Arial, Italic
Formatted: Font: (Default) Times New Roman, Not Italic
Formatted: Left, Line spacing: 1.5 lines
Formatted: Font: (Default) Times New Roman, Not Italic, Subscript
Formatted: Font: (Default) Times New Roman, Not Italic
Formatted: Font: (Default) Times New Roman, Not Italic, Subscript
Formatted: Font: (Default) Times New Roman, Not Italic
Formatted: Font: (Default) Times New

was near solar minimum resulting in the maximum atmospheric influences caused by GCRs. The last previous solar maximum or GCR minimum occured in year 2002. Since the background atmosphere changes significantly from year 2002 to year 2009, it would be confusing to directly compare atmospheric changes between the two years to derive any GCR-caused change. Instead, the annual average percentage change from GCRs was computed for years 2002 and 2009 separately and then differenced from each other to illustrate the GCR-caused change over the solar cycle. The results are given in Figure 7~~6~~ for NO_x (top) and ozone (bottom) using simulations *GCR_SD-W* and *BASE_SD-W*. The computed GCR-induced solar cycle changes from 2002 to 2009 were slightly smaller than those computed for the GCR-maximum (solar minimum) year 2009. The GCR-caused changes are proportional to the GCR-caused ion pair production, which is given in Figure 1 for the years 2002 and 2009. Note that the largest ion pair production near the south pole is over 30 $cm^{-3}s^{-1}$ in 2009 and is nearly 15 $cm^{-3}s^{-1}$ in 2002. Thus, there is a difference of about 15 $cm^{-3}s^{-1}$ from 2002 to 2009 versus a difference of 30 $cm^{-3}s^{-1}$ for 2009 in a comparison without GCRs to with GCRs.

5.2 Time-dependent Total Ozone Changes

The GSFC 2-D model gives fairly similar results to SD-WACCM (compare Figs. 4 and 5) and is significantly faster computationally to use for longer-term simulations. Thus, the GSFC 2-D model was used in several sensitivity study simulations described in Table 1 (and Sect. 4.2) to investigate the longer term GCR-caused changes, particularly focusing on annual average global total ozone (AAGTO) as well as global column ozone in the two regions between 1000 and 100 hPa and between 100 and 1 hPa. The GCR-caused change in ozone in those two regions, separately, and for the entire troposphere and stratosphere (1000 to 1 hPa) is computed for two pairs of scenarios: (1) Fig. 8 (top) shows a comparison of the first pair (A1_GCR_GSFC to A_Base_GSFC), which are simplified representations of the atmosphere with a climatological mean transport (changes daily, but repeats yearly) in both scenarios and a mean GCR input (constant throughout the simulation) in A1_GCR_GSFC; and (2) Fig. 8 (bottom) shows a comparison of the most comprehensive pair (E_GCR_GSFC to E_Base_GSFC), which include interannually varying transport, sulfate aerosol surface area, and solar cycle photon flux variation in both scenarios and an interannually varying GCR input in E_GCR_GSFC.

Formatted: Font: (Default) Times New Roman, Not Italic

Formatted: Left, Line spacing: 1.5 lines

Formatted: Font: (Default) Times New Roman, Not Italic

First, focus on the results intercomparing scenarios A1_GCR_GSFC to A_Base_GSFC (see Fig. 8, top): the GCR-caused column ozone between 1000 and 100 hPa showed an increase from +0.03% up to ~+0.05% over the 1960–2010 time period, driven partly by increases in CH4 over those 51 years. The GCR-caused column ozone between 100 and 1 hPa also showed a time dependent increase, but started in year 1960 at -0.19% ending up at -0.12% in year 2010. The GCR-caused total AAGTO follows the increases in the two regions noted above, starting at -0.16% in year 1960 and increasing to ~-0.07% in year 2010.

Second, intercompare the more complete simulations E_GCR_GSFC to E_Base_GSFC (see Fig. 8, bottom): the GCR-caused column ozone changes between 1000 and 100 hPa showed a significant variation from ~+0.03% to ~+0.07% over the 1960–2010 time period. The GCR-caused column ozone changes between 100 and 1 hPa also showed substantial variation giving -0.23% in 1979 and -0.02% in 1992. The GCR-caused total AAGTO followed these variations, with a low of -0.19% in 1979 and a high of +0.03% in 1992.

~~The GSFC 2-D model gives fairly similar results to SD-WACCM (compare Figures 3 and 4) and is significantly faster computationally to use for longer-term simulations. Thus, the GSFC 2-D model was used in several sensitivity study simulations described in Table 1 (and section 4.2) to investigate the longer-term GCR-caused changes, particularly focusing on annual average global total ozone (AAGTO) as well as global tropospheric and stratospheric column ozone. The GCR-caused change in ozone in the troposphere, stratosphere, and total is computed for two pairs of scenarios: 1) Figure 7 (top) shows a comparison of the first pair (*A1_GCR_GSFC* to *A_Base_GSFC*), which are simplified representations of the atmosphere with a climatological mean transport (changes daily, but repeats yearly) in both scenarios and a mean GCR input (constant throughout the simulation) in *A1_GCR_GSFC*; and 2) Figure 7 (bottom) shows a comparison of the most comprehensive pair (*E_GCR_GSFC* to *E_Base_GSFC*), which include interannually varying transport, sulfate aerosol surface area, and solar cycle photon flux variation in both scenarios and an interannually varying GCR input in *E_GCR_GSFC*.~~

~~First, focus on the results intercomparing scenarios *A1_GCR_GSFC* to *A_Base_GSFC* (see Figure 7, top): The GCR-caused tropospheric column ozone showed an increase from +0.03% up to ~+0.05% over the 1960-2010 time period, likely driven by increases in CH_4 over those 51 years. The GCR-caused stratospheric column ozone also showed a time dependent increase, but started in year 1960 at -0.19% ending up at -0.12% in year 2010. The GCR-~~

Formatted: Font: (Default) Times New Roman, Not Italic

Formatted: Font: (Default) Times New Roman, Not Italic

~~caused total AAGTO follows the tropospheric and stratospheric increases, starting at -0.16% in year 1960 and increasing to ~ -0.07% in year 2010.~~

~~Second, intercompare the more complete simulations *E_GCR_GSFC* to *E_Base_GSFC* (see Figure 7, bottom): The GCR-caused tropospheric column ozone changes showed a significant variation from ~ +0.03% to ~ +0.07% over the 1960-2010 time period. The GCR-caused stratospheric column ozone changes also showed substantial variation giving -0.23% in 1979 and -0.02% in 1992. The GCR-caused total AAGTO followed these variations, with a low of -0.19% in 1979 and a high of +0.03% in 1992.~~

The GCR-caused atmospheric changes are larger at higher latitudes, thus we also compute the annual average polar total ozone (AAPTO). The AAPTO is calculated using the model output only at polar latitudes (60-90 degrees South and 60-90 degrees North) and is given in Figure 9. Both the AAGTO (Figure 8) and the AAPTO (Figure 9) have similar shapes for the total ozone change in the two regions plotted (1000 to 100 hPa and 100 to 1 hPa). In 1960 the AAGTO for the entire troposphere and stratosphere (1000 to 1 hPa) is computed to be -0.13% (see Figure 8, bottom) while the AAPTO is computed to be -0.18% (see Figure 9, bottom). In 2010 the AAGTO for the troposphere and stratosphere is computed to be -0.11% (see Figure 8, bottom) while the AAPTO is computed to be -0.27% (see Figure 9, bottom). Thus, the polar differences tend to be larger by the end than they were at the start of the simulation period.

The impact of five simultaneous atmospheric changes are responsible for the GCR-caused variations in AAGTO observed in Figure 8~~7~~(bottom). These changes are: 1) background total chlorine; 2) sulfate aerosol surface area; 3) solar cycle photon flux variation; 4) solar cycle GCR variation; and 5) interannual transport variability. Background total chlorine increases dramatically from 0.7 to 3.5 ppbv over the 1960-2010 period (Figure 10~~8~~A, Equator, 1 hPa). Volcanoes can add substantially to the aerosol surface area during certain years (especially 1963, 1982, and 1991, see Figure 10~~8~~B). The photon flux varies over the solar cycle and is especially important to the stratosphere at ultraviolet wavelengths. The solar flux variation at 200 nm (up to about 8.5% from solar minimum to maximum) is important for ozone production and is shown in Figure 10~~8~~C. The GCRs vary over the solar cycle as well and the GCR-caused ion pair production is given in Figure 10~~8~~D at 200 hPa and 90^{o}S. The final atmospheric variation is due to the interannual transport variability over the whole time period, which is difficult to illustrate in a line plot (like those given in Figure 10~~8~~).

Formatted: Don't adjust space between Latin and Asian text, Don't adjust space between Asian text and numbers

Formatted: Font: (Default) Times New Roman, Not Italic

5.2.1 Background total chlorine

The smoothest change over the 1960-2010 time period occurred with the amount of background total chlorine. The AAGTO has been computed for the six scenarios (*A_Base_GSFC, A1_GCR_GSFC, A2_GCR_GSFC, B_Base_GSFC, B1_GCR_GSFC, B2_GCR_GSFC*) for use in this analysis. Percentage differences in AAGTO for *A1_GCR_GSFC* compared to *A_Base_GSFC* are shown in Figure 11~~9~~A (black solid line) compared with background total chlorine (red solid line). Note the good correspondence between background total chlorine amount and GCR-caused AAGTO change. Smaller amounts of background total chlorine correlate with larger computed GCR-caused AAGTO decrease and vice versa.

First, this is partly a reflection of the role that chlorine, through the ClO_x catalytic cycle

$$Cl + O_3 \rightarrow ClO + O_2$$
$$ClO + O \rightarrow Cl + O_2$$
$$\text{Net:} \quad O_3 + O \rightarrow O_2 + O_2,$$

has in controlling stratospheric ozone over this time period. At low levels of chlorine, the NO_x catalytic cycle is more important to ozone control. Thus, increases in NO_x, such as caused by GCRs, lead to a more significant ozone response in the 1960s than in the 2000s when the background total chlorine amounts are much higher.

Second, this is also a reflection of the interference of the NO_x family with the ClO_x catalytic cycle through the reaction

$$ClO + NO_2 + M \rightarrow ClONO_2 + M.$$

Increased NO_x amounts caused by GCRs will lead to an increased production of the reservoir constituent, $ClONO_2$, and thus less ozone destruction.

Both of these processes are ongoing in the atmosphere and are reflected in Figure 11~~9~~A, which illustrates most clearly the correlation between the GCR-caused change in ozone and background total chlorine amount.

Figure 11~~9~~B shows the results of the AAGTO computed in *B1_GCR_GSFC* compared to *B_Base_GSFC*. The main difference here is that the model transport changes interannually. There still is a correlation between high background total chlorine amounts and less AAGTO change caused by the GCRs.

Figure 11~~9~~C illustrates the results of a comparison of the AAGTO computed in *A2_GCR_GSFC* compared to *A_Base_GSFC*. Both simulations have the same mean transport imposed over the 51-year time period, however, the GCRs are forced with interannually varying GCRs (see Figure 10~~8~~D). Again, there is a correspondence between the amount of background total chlorine and the GCR-caused AAGTO change.

Finally, Figure 11~~9~~D illustrates the results of a comparison of the AAGTO computed in *B2_GCR_GSFC* compared to *B_Base_GSFC*. Both simulations have interannual transport and the simulation with GCRs (*B2_GCR_GSFC*) includes the interannual variation of GCRs. Although there is clearly more year-to-year variability, it is apparent that higher background total chlorine levels lead to less GCR-caused ozone changes.

5.2.2 Aerosol surface area

The aerosol surface area varies dramatically over the 1960-2010 time period. Volcanoes in years 1963, 1982, and 1991 caused large increases in the aerosol surface area. Enhanced aerosol surface area results in an increase in heterogeneous reactions on the sulfate aerosols. In particular, the reaction

$$N_2O_5 + H_2O \rightarrow 2HNO_3$$

proceeds rapidly, taking the more active NO_x constituents and producing the less active HNO_3 reservoir constituent. The result of this is that NO_x production from any source is less efficient. A comparison of the AAGTO computed in *C_GCR_GSFC* compared to *C_Base_GSFC* is shown in Figure 12~~0~~. This shows that the GCRs cause a less negative change (even positive in 1992-3) in AAGTO during the years of enhanced aerosol surface area.

5.2.3 Solar cycle photon variation

The sun not only influences the GCR flux over a solar cycle, but it also shows a significant variation in solar photons and solar particles (electrons, protons and other particles). The photon flux variation and its impact on the GCR effect will be addressed here. However, it is outside the scope of this paper to discuss the influence of solar energetic particles (e.g., protons, other ions, and electrons) on the GCR-caused atmospheric influence.

The solar cycle variation led to changes in the photon flux, especially at the X-ray, extreme ultraviolet, and ultraviolet wavelengths. In particular, the stratosphere is greatly influenced by photons at ultraviolet wavelengths (e.g., 200 nm photons are important in producing

ozone) and a variation of up to about 8.5% from solar minimum to maximum was shown in Figure 108C. A comparison of the AAGTO computed in *D_GCR_GSFC* was compared to *D_Base_GSFC*. These simulations isolated the impact of the solar cycle photon variation on the GCR influence. Only a very minor change (+/- 0.004% in AAGTO) was found to be forced by the solar cycle photon flux variation (not shown).

5.2.4 GCR interannual and solar cycle driven variation

The GCRs vary from year-to-year, influenced primarily by the strength of the solar magnetic field. The GCR variation (given in ion pair production) can be as large as a factor of two at the poles (see Figure 108D). Most of the impact from GCRs is in the polar lower stratosphere/ upper troposphere, since the GCR caused ionization rates peak there (see Figure 1). The residence time for constituents in the lower stratosphere is long (~1 year or so, which is driven by the transport) as is the photochemical time constant for odd oxygen (essentially ozone) in this region (e.g., see Figure 5.3, Brasseur and Solomon, 1995), thus the computed impact of the GCRs on the atmosphere will be a time-lagged average of the GCR input. The AAGTO shown in Figure 119C was differenced from that shown in Figure 119A in order to compute the change caused by the interannual GCR variation. This interannually-driven GCR change in AAGTO is represented by the black line in Figure 1311. The red line in Figure 1311 is a two-year boxcar (running) average of the GCR ion pair production (in $cm^{-3}s^{-1}$) at 200 hPa and 90°S with a one-year lag and appears to be an anti-correlation of the AAGTO change. Thus, the impact of the interannual variation in the GCRs with an imposed one-year time lag and two-year average can represent the computed AAGTO change fairly well.

5.2.5 Interannual transport variation

The interannual transport variation drives changes in the impact of the GCRs on the AAGTO. This interannual behavior is best observed in Figure 119B, where the mean GCRs are imposed continuously over the entire 51-year time period. Variations of up to ~0.04% in the GCR-caused AAGTO impact are computed over a couple of years or so. However as noted in section 5.3.1, the strong correlation between high background total chlorine amounts and less AAGTO change caused by the GCRs dominates so that the interannual transport changes have only a very small effect on the time-dependent GCR-induced AAGTO impact.

5.3 NO_y Production

The total NO_y produced per year from GCRs was compared with that from other sources. GSFC 2-D model calculations show that N_2O oxidation ($N_2O + O(^1D) \rightarrow NO + NO$) produce 43.5-55.7 GigaMoles of NO_y with the vast majority (greater than 90%) produced in the stratosphere. GCRs were computed to produce 3.1-6.4 GigaMoles of NO_y, with 40-50% of that produced in the stratosphere. Thus, GCRs can be responsible for as much as 14% of the total NO_y production, however on average, GCRs produce about 3-6% of stratospheric NO_y in any given year. This is somewhat less than that found by Vitt and Jackman (1996), who computed that GCRs were responsible for 9-12% of the total stratospheric NO_y produced per year. The Vitt and Jackman (1996) computations used ion pair production rates from a parameterization based on yearly averaged sunspot number from Nicolet (1975), which are generally larger than those GCR-caused ion pair production rates computed with the more recent NAIRAS model (discussed in section 2).

6 Conclusions

Two global models, SD-WACCM and GSFC 2-D, were used to study the atmospheric impact of GCRs over the 1960-2010 time period. The largest atmospheric impacts occurred in the NO_x constituents, which had maximum GCR-caused increases of 4-15% in the Southern polar troposphere. There were associated ozone increases of 1-2% correlated with these NO_x enhancements. The lower stratosphere was also impacted with computed NO_x increases of ~1-6% causing associated ozone decreases of 0.2-1%. GCR-caused decreases of AAGTO were computed to be 0.2% or less with GCR-caused tropospheric column ozone increases of 0.08% or less and GCR-caused stratospheric column ozone decreases of 0.23% or less. There appears to be a time lag of about a year between the GCR-caused NO_x production and the resultant AAGTO change. This is consistent with the long residence and photochemical time constant of ozone in the lower stratosphere. The impact of GCRs has a strong correlation with the atmospheric chlorine loading, sulfate aerosol loading, and solar cycle variation. GCRs cause larger atmospheric impacts with less chlorine loading, less sulfate aerosol loading, and for years closer to solar minimum.

Acknowledgements

CHJ, DRM, DEK, CJM, and ELF thank the NASA Headquarters Living With a Star Targeted Research and Technology Program for support during the time that this manuscript was written. CHJ and ELF were also supported by the NASA Headquarters Atmospheric Composition Modeling and Analysis Program. The National Center for Atmospheric

Research (NCAR) is sponsored by the U.S. National Science Foundation. WACCM is a component of the Community Earth System Model (CESM), which is supported by the National Science Foundation (NSF) and the Office of Science of the U.S. Department of Energy. Computing resources were provided by NCAR's Climate Simulation Laboratory, sponsored by NSF and other agencies. This research was enabled by the computational and storage resources of NCAR's Computational and Information System Laboratory (CISL).

References

Badhwar, G. D. and O'Neill, P. M.: An improved model of galactic cosmic radiation for space exploration missions, *Nuclear Tracks Radiat. Mea*, **20,** 403-410, 1992.

Badhwar, G. D. and O'Neill, P. M.: Long term modulation of galactic cosmic radiation and its model for space exploration, *Adv. Space Res.*, **14**, 749-757, 1994.

Badhwar, G. D. and O'Neill, P. M.: Galactic cosmic radiation model and its applications, *Adv. Space Res.*, **17**, 7-17, 1996.

Brasseur, G., and Solomon, S.: Aeronomy of the Middle Atmosphere: Chemistry and Physics of the Stratosphere and Mesosphere, D. Reidel Publishing Company, Dordrecht, The Netherlands, 1995.

Calisto, M., Usoskin, I., Rozanov, E., and Peter, T.: Influence of Galactic Cosmic Rays on atmospheric composition and dynamics, *Atmos. Chem. Phys.*, **11**, 4547-4556, 2011.

~~Calogovic, J., Albert, C., Arnold, F., Beer, J., Desorgher, L., and Flueckiger, E. O.: Sudden cosmic ray decreases: No change of global cloud cover, *Geophys. Res. Lett.*, *37*, L03802, doi:10.1029/2009GL041327, 2010.~~

Considine, D. B., Douglass, A. R., and Jackman, C. H.: Effects of a polar stratospheric cloud parameterization on ozone depletion due to stratospheric aircraft in a two-dimensional model, *J. Geophys. Res.*, *99*, 18,879– 18,894, 1994.

Douglass, A. R., Jackman, C. H., and Stolarski, R. S.: Comparison of model results transporting the odd nitrogen family with results transporting separate odd nitrogen species, *J. Geophys. Res.*, *94*, 9862-9872, 1989.

Duncan, B.N., Strahan, S.E., Yoshida, Y., Steenrod, S.D., and Livesey, N.: Model study of the cross-tropopause transport of biomass burning pollution, *Atmos. Chem. Phys.*, *7*, 3713–3736, doi:10.5194/acp-7-3713-2007, 2007.

Emmons, L. K., Walters, S., Hess, P. G., Lamarque, J.-F., Pfister, G. G., Fillmore, D., Granier, C., Guenther, A., Kinnison, D., Laepple, T., Orlando, J., Tie, X., Tyndall, G., Wiedinmyer, C., Baughcum, S. L., and Kloster, S.: Description and evaluation of the Model for Ozone and Related chemical Tracers, version 4 (MOZART-4), *Geosci. Model Dev.*, *3*, 43–67, doi:10.5194/gmd-3-43-2010, 2010.

Eyring, V., Lamarque, J.-F., Hess, P., Arfeuille, F., Bowman, K., Chipperfield, M., Duncan, B., Fiore, A., Gettelman, A., Giorgetta, M., Granier, C., Hegglin, M., Kinnison, D., Kunze, M., Langematz, U., Luo, B., Martin, R., Matthes, K., Newman, P., Peter, T., Robock, A., Ryerson, T., Saiz-Lopez, A., Salawitch, R., Schultz, M., Shepherd, T. G., Shindell, D., Staehelin, J., Tegtmeier, S., Thomason, L., Tilmes, S., Vernier, J.-P., Waugh, D. W., and Young, P. J.: Overview of IGAC/SPARC Chemistry-Climate Model Initiative (CCMI) Community Simulations in Support of Upcoming Ozone and Climate Assessments, SPARC newsletter, n40, pg48-66, Zurich, Switzerland, January 2013.

Finlay, C. C., Maus, S., Beggan, C. D., Bondar, T. N., Chambodut, A., Chernova, T. A.,Chulliat, A., Golovkov, V. P., Hamilton, B., Hamoudi, M., Holme, R., Hulot, G., Kuang, W., Langlais, B., Lesur, V., Lowes, F. J., Lühr, H., Macmillan, S., Mandea, M., McLean, S., Manoj, C., Menvielle, M., Michaelis, I., Olsen, N., Rauberg, J., Rother, M., Sabaka, T. J., Tangborn, A.,Tøffner-Clausen, L.,Thébault, E.,Thomson, A. W. P., Wardinski, I., Wei, Z., and Zvereva, T. I.: International Geomagnetic Reference Field: the eleventh generation, *Geophysical Journal International*, *183*, 1216-1230, doi10.1111/j.1365-246X.2010.04804, 2010.

Formatted: Font: (Default) Times New Roman, Not Italic

Formatted: Add space between paragraphs of the same style, Widow/Orphan control, Don't keep with next, Don't keep lines together

Formatted: Font: (Default) Times New Roman, Not Italic

Formatted: Font: (Default) Times New

Formatted: Font: (Default) Times New Roman, Not Italic

Fleming, E. L., Jackman, C. H., Considine, D. B., and Stolarski, R. S.: Simulation of stratospheric tracers using an improved empirically based two-dimensional model transport formulation, *J. Geophys. Res., 104*, 23911-23934, 1999.

Fleming, E. L., Jackman, C. H., Weisenstein, D. K., and Ko, M. K. W.: The impact of inter-annual variability on multidecadal total ozone simulations, *J. Geophys. Res., 112*, D10310, doi:10.1029/2006JD007953, 2007.

Fleming, E. L., Jackman, C. H., Stolarski, R. S., and Douglass, A. R.: A model study of the impact of source gas changes on the stratosphere for 1850-2100, *Atmos. Chem. Phys. 11*, 8515-8541, 2011.

Fleming, E. L., George, C., Heard, D. E., Jackman, C. H., Kurylo, M. J., Mellouki, W., Orkin, V. L., Swartz, W. H., Wallington, T. J., Wine, P. H., and Burkholder, J. B.: The impact of current CH_4 and N_2O atmospheric loss process uncertainties on calculated ozone abundances and trends, *J. Geophys. Res. Atmos., 120*, 5267–5293, doi:10.1002/2014JD022067, 2015.

Garcia, R. R., Solomon, S., Roble, R. G., and Rusch, D. W.: A numerical response of the middle atmosphere to the 11-year solar cycle, *Planet. Space Sci., 32,* 411-423, 1984.

~~Gronoff, G. P., R. B. Norman, C. J. Mertens: Computation of cosmic ray ionization and dose at Mars. I: A comparison of HZETRN and Planetocosimes for protons and alpha particles, *Adv. Space Res.*, 55, 1799-1805, 2015.~~

Jackman, C. H.: Effects of energetic particles on minor constituents of the middle atmosphere, *J. Geomag. Geoelectr., 43, Suppl.,* 637-646, 1991.

Jackman, C. H.: Energetic particle influences on NO_y and Ozone in the middle atmosphere, *Interactions Between Global Climate Subsystems, The Legacy of Hann, Geophysical Monograph 75, IUGG Volume 15,* 131-139, 1993.

Jackman, C. H., Frederick, J. E., and Stolarski, R. S.: Production of odd nitrogen in the stratosphere and mesosphere: An intercomparison of source strengths, *J. Geophys. Res., 85,* 7495-7505, 1980.

Jackman, C. H., Guthrie, P. D., and Kaye, J. A.: An intercomparison of nitrogen-containing species in Nimbus 7 LIMS and SAMS data, *J. Geophys. Res., 92*, 995-1008, 1987.

Jackman, C. H., Douglass, A. R., Rood, R. B., McPeters, R. D., and Meade, P. E.: Effect of Solar Proton Events on the Middle Atmosphere During the Past Two Solar Cycles as Computed Using a Two-dimensional Model, *J. Geophys. Res., 95*, 7417-7428, 1990.

Jackman, C. H., Fleming, E. L., Chandra, S., Considine, D. B., and Rosenfield, J. E.: Past, present, and future modeled ozone trends with comparisons to observed trends, *J. Geophys. Res., 101*, 28753-28767, 1996.

Jackman, C. H., DeLand, M. T., Labow, G. J., Fleming, E. L., Weisenstein, D. K., Ko, M. K. W., Sinnhuber, M., and Russell, J. M.: Neutral atmospheric influences of the solar proton events in October-November 2003, *J. Geophys. Res., 110*, A09S27, doi:10.1029/2004JA010888, 2005.

Kalnay, E., Kanamitsu, M., Kistler, R., Collins, W., Deaven, D., Gandin, L., Iredell, M., Saha, S., White, G., Woollen, J., Zhu, Y., Chelliah, M., Ebizusaki, W., Higgins, W., Janowiak, J., Mo, K. C., Ropelewski, C., Wang, J., Leetmaa, A., Reynolds, R., Jenne, R., and Joseph, D.: The NCEP/NCAR 40-year reanalysis project, *Bull. Am. Meteor. Soc., 77*, 437-471, 1996.

Kistler, R., Collins, W., Saha, S., White, G., Woollen, J., Kalnay, E., Chelliah, M., Ebizusaki, W., Kanamitsu, M., Kousky, V., van den Dool, H., Jenne, R., and Fiorino, M.: The NCEP-NCAR 50-year reanalysis: Monthly means CD-ROM and documentation, *Bull. Am. Meteor. Soc., 82,* 247-267, 2001.

Kinnison, D. E., Brasseur, G. P., Walters, S., Garcia, R. R., Marsh, D. R., Sassi, F., Harvey, V. L., Randall, C. E., Emmons, L., Lamarque, J. F., Hess, P., Orlando, J. J., Tie, X. X., Randel, W., Pan, L. L., Gettelman, A., Granier, C., Diehl, T., Niemeier, U., and Simmons, A. J.: Sensitivity of chemical tracers to meteorological parameters in theMOZART-3 chemical transport model, *J. Geophys. Res.*, *112*, D20302, doi:10.1029/2006JD007879, 2007.

~~Ko, M. K. W., Newman, P. A., Reimann, S., and Strahan, S. E.: SPARC (Stratosphere-Trospophere Processes and their Role in Climate), Lifetimes of Stratospheric Ozone-Depleting Substances, Their Replacements, and Related Species – Report No. 6., SPARC Office, Zurich, Switzerland, 2013.~~

Krivolutsky, A. A., Kuminov, A. A., and Repnev, A. I.: Effects of Cosmic Rays on the Earth's Ozonosphere: A Review, *Geomagnetism and Aeronomy*, **39**, 271-282, 1999.

Krivolutsky, A. A., Bazilevskaya, G. A., Vyushkova, T. Y., and Knyazeva, G. V.: Long-term tropospheric variations of ozone content caused by galactic cosmic ray influence, *Adv. Space Res., 27,* 2019-2024, 2001.

Krivolutsky, A., Bazilevskaya, G., Vyushkova, T., and Knyazeva, G.: Influence of cosmic rays on chemical composition of the atmosphere: data analysis and photochemical modeling, *Phys. Chem. Earth*, **27**, 471-476, 2002.

Kunz, A., Pan, L., Konopka, P., Kinnison, D. E., and Tilmes, S.: Chemical and dynamical discontinuity at the extratropical tropopause based on START08 and WACCM analysis, *J. Geophys. Res.*, *116*, D24302, doi:10.1029/2011JD016686, 2011.

Lamarque, J.-F., Emmons, L. K., Hess, P. G., Kinnison, D. E., Tilmes, S., Vitt, F., Heald, C. L., Holland, E. A., Lauritzen, P. H., Neu, J., Orlando, J. J., Rasch, P. J., and Tyndall, G. K.: CAM-chem: Description and evaluation of interactive atmospheric chemistry in the Community Earth System Model, *Geosci. Model Dev.*, *5*, 369–411, doi:10.5194/gmd-5-369-2012, 2012.

Legrand, M. R., Stordal, F., Isaksen, I. S. A., and Rognerud, B.: A model study of the stratospheric budget of odd nitrogen, including effects of solar cycle variations, *Tellus, 41B,* 413-426, 1989.

McPeters, R.D., Labow, G.J., and Logan, J.A.: Ozone climatological profiles for satellite retrieval algorithms, *J. Geophys. Res., 112*, D05308, doi:10.1029/2005JD006823, 2007.

Mertens, C. J., Kress, B. T., Wiltberger, M., Tobiska, W. K., Grajewski, B., and Xu, X.: Atmospheric ionizing radiation from galactic and solar cosmic rays, Current Topics in Ionizing Radiation Research, Edited by Mitsuru Nenoi, InTech Publisher (ISBN 978-953-51-0196-3), 2012.

Mertens, C. J., Meier, M. M., Brown, S., Norman, R. B., and Xu, X.: NAIRAS aircraft radiation model development, dose climatology, and initial validation, *Space Weather*, **11**, 603-635, doi:10.1002/swe.20100, 2013.

Mironova, I. A., Aplin, K. L., Arnold, F., Bazilevskaya, G. A., Harrison, R. G., Krivolutsky, A. A., Nicoll, K. A., Rozanov, E. V., Turunen, E., Usoskin, I. G.: Energetic Particle Influence on the Earth's Atmosphere, *Space Sci. Rev., 194*, 1–96, 2015.

Müller, R., and Crutzen, P. J.: A possible role of galactic cosmic rays in chlorine activation during polar night, *J. Geophys. Res.*, *98,* 20483-20490, 1993.

~~Neher, H. V.: Cosmic-ray particles that changed from 1954 to 1958 to 1965, *J. Geophys. Res., 72*, 1527-1539, 1967.~~

Nicolet, M.: On the production of nitric oxide by cosmic rays in the mesosphere and stratosphere, *Planet. Space Sci., 23,* 637-649, 1975.

Formatted: Font: (Default) Times New Roman, Not Italic

Formatted: Font: (Default) Times New Roman, Not Italic

Formatted: Indent: Left: 0", Hanging: 0.49"

Formatted: Font color: Black, German (Germany)

Formatted: Font: (Default) Times New Roman, Not Italic

Formatted: Font: (Default) Times New Roman, Not Italic

Formatted: Font: (Default) Times New

Formatted: Font: (Default) Times New Roman, Not Italic

Norman, R. B., Blattnig, S. R., De Angelis, G., Badavi, F. F., and Norbury, J. W.: Deterministic pion and muon tranport in Earth's atmosphere, *Adv. Space Res., 50*, 146-155, 2012.

Norman, R. B., Slaba, T. C., and Blattnig, S. R.: An extension of HZETRN for cosmic ray initiated electromagnetic cascades, *Adv. Space Res., 51*, 2251-2260, 2013.

O'Neill, P. M. : Badhwar-O'Neill 2010 galactic cosmic ray flux model – Revised, *IEEE Trans. Nucl. Sci.*, 57(6), 3148-3153, 2010.

Picone, J. M., Hedin, A. E., Drob, D. P., and Aikin, A. C.: NRLMSIS-00 empirical model of the atmosphere: Statistical comparisons and scientific issues, *J. Geophys. Res., 107(A12)*, 1468, 10/1029/2002JA009430, 2002.

Porter, H. S., Jackman, C. H., and Green, A. E. S.: Efficiencies for production of atomic nitrogen and oxygen by relativistic proton impact in air, *J. Chem. Phys., 65*, 154-167, 1976.

Rienecker, M. M., Suarez, M. J., Gelaro, R., Todling, R., Bacmeister, J., Liu, E., Bosilovich, G., Schubert, S. D., Takacs, L., Kim, G.-K., Bloom, S., Chen, J., Collins, D., Conaty, A., da Silva, A., Gu, W., Joiner, J., Koster, R. D., Lucchesi, R., Molod, A., Owens, T., Pawson, S., Pegion, P., Redder, C. R., Reichle, R., Robertson, F. R., Ruddick, A. G., Sienkiewicz, M., and Woollen, J.: MERRA: NASA's modern-era retrospective analysis for research and applications, *J. Climate*, *24*, 3624–3648, doi:10.1175/JCLI-D-11-00015.1, 2011.

Ruderman, M. A., and Chamberlain, J. W.: Origin of the sunspot modulation of ozone: Its implications for stratospheric NO injection, *Planet. Space Sci., 23*, 247-268, 1975.

Sander, S. P., Abbatt, J., Barker, J. R., Burkholder, J. B., Friedl, R. R., Golden, D. M., Huie, R. E., Kolb, C. E., Kurylo, M. J., Moortgat, G. K., Orkin, V. L., and Wine, P. H.: Chemical kinetics and photochemical data for use in atmospheric studies, Evaluation Number 17, JPL Publication 10-6., Pasadena, California, 2011.

Semeniuk, K., Fomichev, V. I., McConnell, J. C., Fu, C., Melo, S. M. L., and Usoskin, I. G.: Middle atmosphere response to the solar cycle in irradiance and ionizing particle precipitation, *Atmos. Chem. Phys.*, **11**, 5045-5077, 2011.

Slaba, T. C., Blattnig, S. R., Reddell, B., Bahadori, A., Norman, R. B., and Badavi, F. F.: Pion and electromagnetic contribution to dose: Comparisons of HZETRN to Monte Carlo results and ISS data, *Adv. Space Res., 52*, 62-78, 2013.

Smart, D. F. and Shea, M. A.: Geomagnetic cutoffs: A review for space dosimetry calculations, *Adv. Space Res., 14(10)*, 10,787-10,796, 1994.

Smart, D. F. and Shea, M. A.: A review of geomagnetic cutoff rigidities for earth-orbiting spacecraft, *Adv. Space Res., 36*, 2012-2020, 2005.

Solomon, S., Rusch, D. W., Gerard, J.-C., Reid, G. C., and Crutzen, P. J.: The effect of particle precipitation events on the neutral and ion chemistry of the middle atmosphere, 2, Odd hydrogen, *Planet. Space Sci., 29*, 885-892, 1981.

Solomon, S., Kinnison**,** D., Bandoro, J., Garcia, R.: Simulations of Polar Ozone Depletion: An Update, *J. Geophys. Res.*, 120, 7958-7974, doi:10.1002/2015JD023365, 2015.

SPARC (Stratosphere-Trospophere Processes and their Role in Climate) Report on the Lifetimes of Stratospheric Ozone-Depleting Substances, Their Replacements, and Related Species: Ko, M. K. W., Newman, P. A., Reimann, S., and Strahan, S. E. (Eds.), SPARC Report No. 6., WCRP-15/2013, [Available at http://www.sparc-climate.org/publications/sparc-reports/sparc-report-no6/], SPARC Office, Zurich, Switzerland, 2013.

Spivakovsky, C. M., Logan, J. A., Montzka, S. A., Balkanski, Y. J., Foreman-Fowler, M., Jones, D. B. A., Horowitz, L. W., Fusco, A. C., Brenninkmeijer, C. A. M., Prather, M.

Formatted: Font: (Default) Times New Roman, Not Italic

Formatted: Font: (Default) Times New Roman, Not Italic

Formatted: Left, Indent: Left: 0", Hanging: 0.49", Space Before: 0 pt

Formatted: Font: (Default) Times New

Formatted: Font: (Default) Times New Roman, Not Italic

Formatted: Font: (Default) Times New Roman, Not Italic

Formatted: Font: (Default) Times New Roman, Not Italic

Formatted: Normal, Don't adjust space between Latin and Asian text, Don't adjust space between Asian text and numbers

Formatted: Font: (Default) Times New

Formatted: Font: (Default) Times New Roman, Not Italic

Formatted: Font:

Formatted: Font: (Default) Times New Roman, Not Italic

Formatted: Normal, Don't adjust space between Latin and Asian text, Don't adjust space between Asian text and numbers

Formatted: Font: (Default) Times New Roman, Not Italic

Formatted: Font: (Default) Times New

Formatted: Font: (Default) Times New Roman, Not Italic

Formatted: Font:

Formatted: Font: (Default) Times New Roman, Not Italic

Formatted: Left, Indent: Left: 0", Hanging: 0.49", Space Before: 0 pt

Formatted: Font: (Default) Times New Roman, Not Italic

Formatted: Font: (Default) Times New

Formatted: Font: (Default) Times New Roman, Not Italic

Formatted: Font: (Default) Times New Roman, Not Italic

Formatted: Font: (Default) Times New

Formatted: Font: (Default) Times New Roman, Not Italic

Formatted: Don't adjust space between Latin and Asian text, Don't adjust space between Asian text and numbers

Formatted ... [1]

Formatted: Font: (Default) Times New

Formatted ... [2]

Formatted: Font:

Formatted ... [3]

J., Wofsy, S. C., and McElroy, M. B.: Three-dimensional climatological distribution of tropospheric OH: Update and evaluation, J. Geophys. Res., 105, 8931-8980, doi:10.1029/1999JD901006, 2000.

Strahan, S. E., Duncan, B. N., and Hoor, P.: Observationally derived transport diagnostics for the lowermost stratosphere and their application to the GMI chemistry and transport model, *Atmos. Chem. Phys., 7*, 2435–2445, doi:10.5194/acp-7-2435-2007, 2007.

Strode, S.A., Rodriguez, J. M., Logan, J. A., Cooper, O. R., Witte, J. C., Lamsal, L. N., Damon, M., Van Aartsen, B., Steenrod, S. D., and Strahan, S. E.: Trends and variability in surface ozone over the United States, *J. Geophys. Res. Atmos. 120,* 9020-9042, doi:10.1002/2014JD022784, 2015.

Thorne, R. M.: The importance of energetic particle precipitation on the chemical composition of the middle atmosphere, *Pure Appl. Geophys., 118,* 128-151, 1980.

Usoskin, I. G., Kovaltsov, G. A., and Mironova, I. A.; Cosmic ray induced ionization model CRAC:CRII; An extension to the upper atmosphere, *J. Geophys. Res., 115,* D10302, doi:10.1029/2009JD013142, 2010.

Vitt, F. M., and Jackman, C. H.: A comparison of sources of odd nitrogen production from 1974 through 1993 in the Earth's middle atmosphere as calculated using a two-dimensional model, *J. Geophys. Res.*, *101*, 6729-6739, 1996.

Vitt, F. M., Armstrong, T. P., Cravens, T. E., Dreschhoff, G. A. M., Jackman, C. H., and Laird, C. M.: Computed contributions to odd nitrogen concentrations in the Earth's polar middle atmosphere by energetic charged particles, *J. Atmos. Solar-Terr. Phys., 62*, 669-683, 2000.

Warneck, P.: Cosmic radiation as a source of odd nitrogen in the stratosphere, *J. Geophys. Res.*, *77*, 6589-6591, 1972.

Wegner, T., Kinnison, D. E., Garcia, R. R., and Solomon, S.: Simulation of polar stratospheric clouds in the specified dynamics version of the whole atmosphere community climate model, *J. Geophys. Res. Atmos.*, *118*, 4991–5002, doi:10.1002/jgrd.50415, 2013.

WMO (World Meteorological Organization): Scientific Assessment of Ozone Depletion: 2014, Global Ozone Research and Monitoring Project-Report No. 55, Geneva, Switzerland, 2014.

Formatted: Font: (Default) Times New Roman, Not Italic

1

Table 1. **Description of model simulations**				
Simulation Designation	***Model***	***Time Period (Years)***	***Include GCRs***	***Other Information***
Base_SD-W	SD-WACCM	2000-2009	No	Interannual MERRA Transport No Sulfate Aerosol (SA) Variation No Solar Cycle (SC) Photon Flux (PF) Variation
GCR_SD-W	SD-WACCM	2000-2009	Yes, Interannually Varying	Interannual MERRA Transport No SA Var., No SC PF Var.
A_Base_GSFC	GSFC 2-D	1960-2010	No	Climatological Averaged Transport No SA Var., No SC PF Var.
B_Base_GSFC	GSFC 2-D	1960-2010	No	Interannual Transport No SA Var., No SC PF Var.
C_Base_GSFC	GSFC 2-D	1960-2010	No	Climatological Averaged Transport SA Var., No SC PF Var.
D_Base_GSFC	GSFC 2-D	1960-2010	No	Climatological Averaged Transport No SA Var., SC PF Var.
E_Base_GSFC	GSFC 2-D	1960-2010	No	Interannual Transport SA Var., SC PF Var.
A1_GCR_GSFC	GSFC 2-D	1960-2010	Yes, Mean of Values	Climatological Averaged Transport No SA Var., No SC PF Var.
A2_GCR_GSFC	GSFC 2-D	1960-2010	Yes, Interannually Varying	Climatological Averaged Transport No SA Var., No SC PF Var.
B1_GCR_GSFC	GSFC 2-D	1960-2010	Yes, Mean of Values	Interannual Transport No SA Var., No SC PF Var.
B2_GCR_GSFC	GSFC 2-D	1960-2010	Yes, Interannually Varying	Interannual Transport No SA Var., No SC PF Var.
C_GCR_GSFC	GSFC 2-D	1960-2010	Yes, Mean of Values	Climatological Averaged Transport SA Var., No SC PF Var.
D_GCR_GSFC	GSFC 2-D	1960-2010	Yes, Mean of Values	Climatological Averaged Transport No SA Var., SC PF Var.
E_GCR_GSFC	GSFC 2-D	1960-2010	Yes, Interannually Varying	Interannual Transport SA Var., SC PF Var.

2

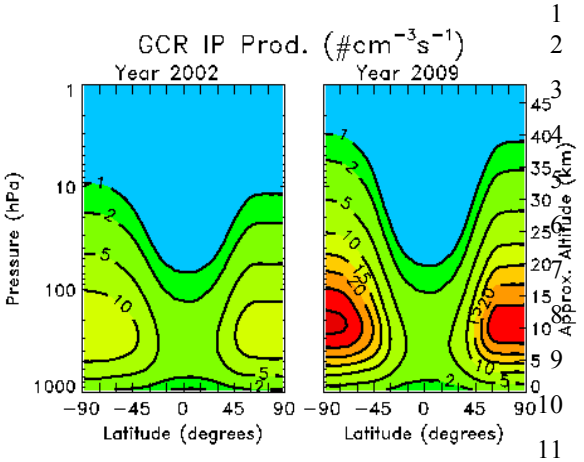

Figure 1. NAIRAS model computed GCR annual average ionization rates for years 2002 (left) and 2009 (right). Contour intervals are 1, 2, 5, 10, 15, 20, 25, and 30 (#cm^{-3} s^{-1}).

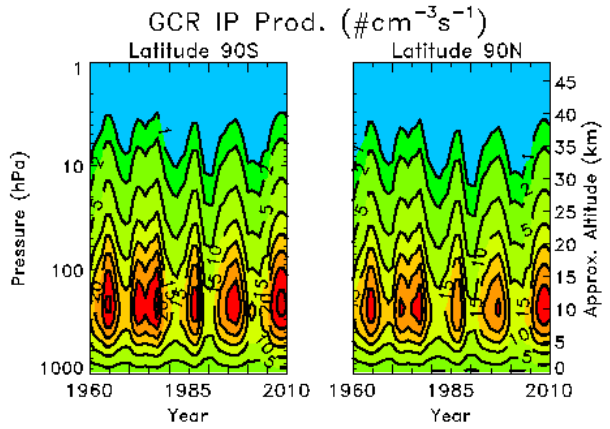

Figure 2. NAIRAS model computed galactic cosmic ray annual average ionization rates at 90°S (left) and 90°N (right) over the time period 1960-2010. Contour intervals are 1, 2, 5, 10, 15, 20, 25, and 30 (#cm^{-3} s^{-1}).

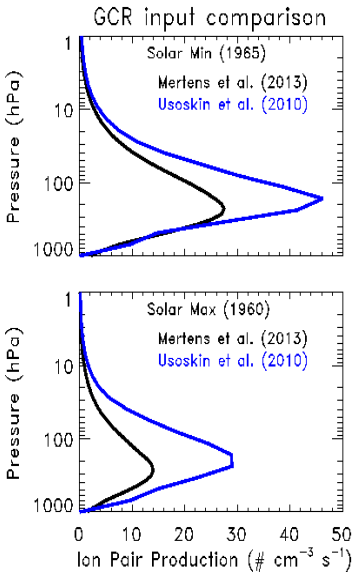

Figure 3. NAIRAS model computed galactic cosmic ray annual average ionization rates (Mertens et al., 2013) compared to those given in Usoskin et al. (2010) for solar minimum (1965, top plot) and solar maximum (1960, bottom plot).

Formatted: Left, Line spacing: 1.5 lines

Formatted: Font: (Default) Times New Roman, Not Italic

Formatted: Font: (Default) Times New Roman, Bold, Not Italic

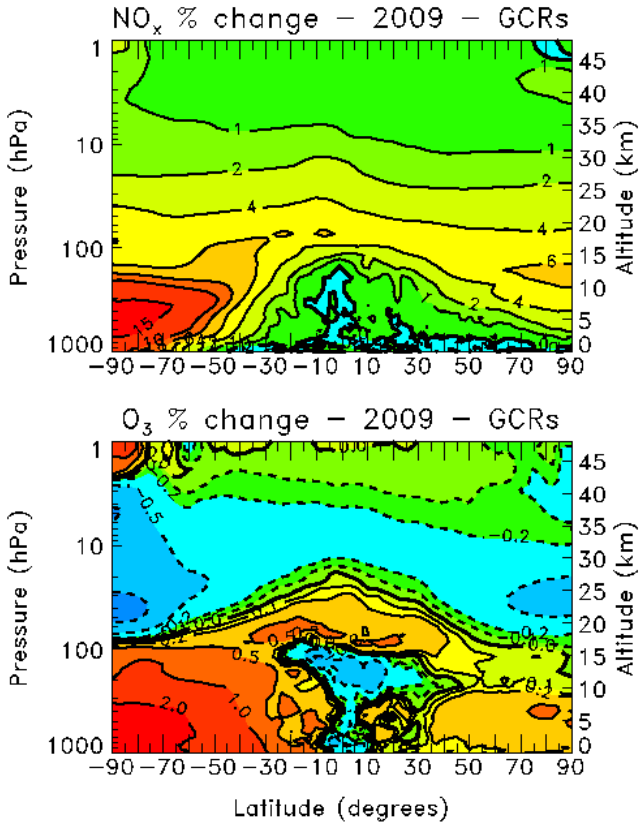

Figure 43. Annual average percentage change for year 2009 in zonal mean NO_x (top) and ozone (bottom) due to GCRs in the SD-WACCM (simulation *Base_SD_W* compared to *GCR_SD_W*). The contour intervals for the NO_x changes are 0, 1, 2, 4, 6, 8, 10, and 15%. The contour intervals for the ozone changes are -1, -.5, -.2, -.1, 0, .1, .2, .5, 1, and 2%.

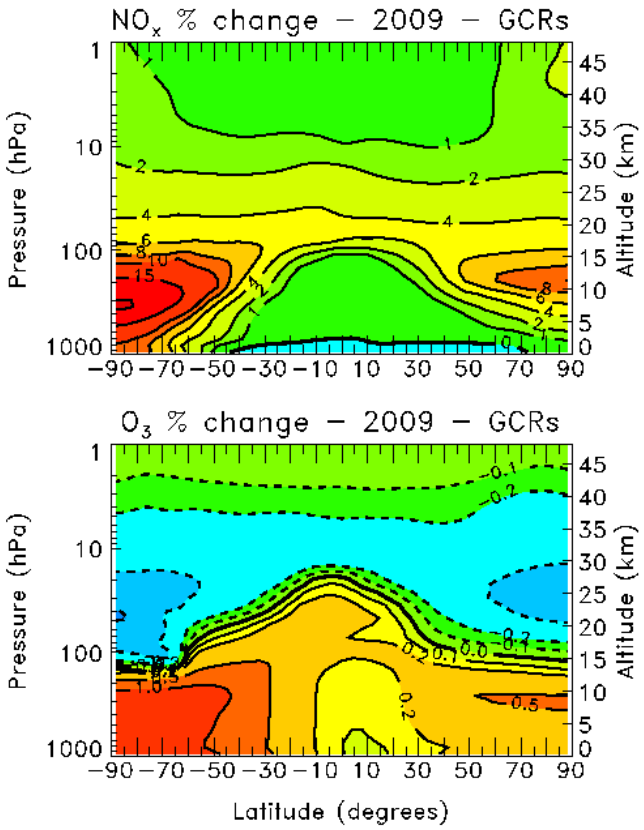

Figure 54. Annual average percentage change for year 2009 in zonal mean NO_x (top) and ozone (bottom) due to GCRs in the GSFC 2-D model (simulation *B2_GCR_GSFC* compared to *B_Base_GSFC*). The contour intervals for the NO_x changes are 0, 1, 2, 4, 6, 8, 10, 15, and 20%. The contour intervals for the ozone changes are -1, -.5, -.2, -.1, 0, .1, .2, .5, and 1%.

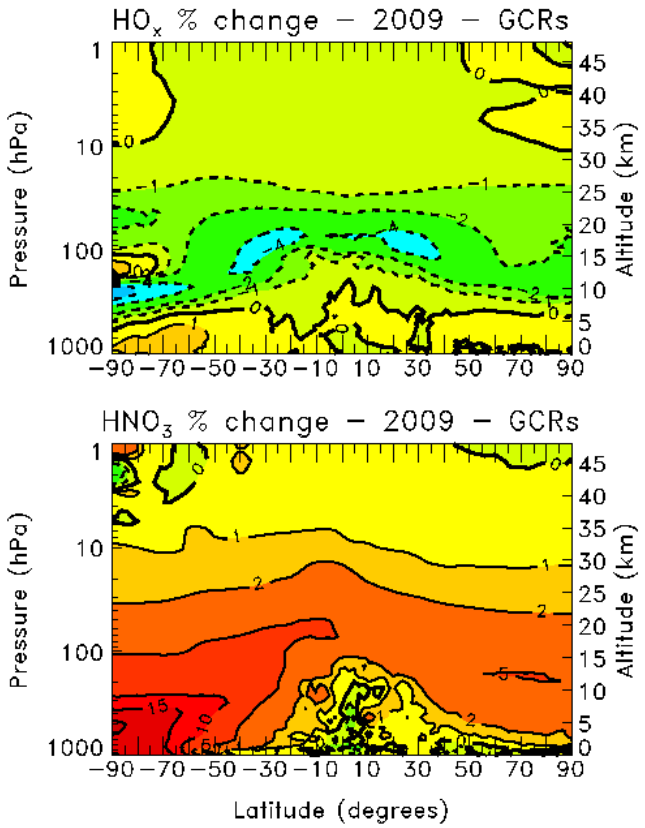

Figure 6~~5~~. Annual average percentage change for year 2009 in zonal mean HO_x (top) and HNO_3 (bottom) due to GCRs in the SD-WACCM (simulation *Base_SD_W* compared to *GCR_SD_W*). The contour intervals for the HO_x changes are -6, -4, -2, -1, 0, and 1%. The contour intervals for the HNO_3 are -1, 0, 1, 2, 5, 10, 15, and 20%.

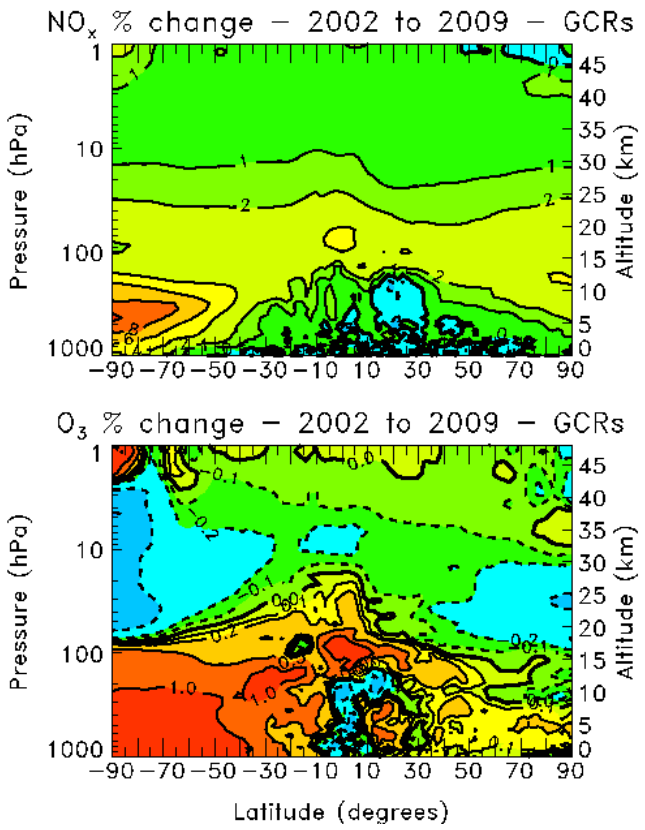

Figure 7~~6~~. Annual average percentage change from year 2002 (solar maximum) to 2009 (solar minimum) in zonal mean NO_x (top) and ozone (bottom) in the SD-WACCM. Simulations *GCR_SD-W* and *Base_SD-W* were used for this comparison. The annual average percentage change from GCRs was computed for years 2002 and 2009 separately and then differenced from each other. The contour intervals for the NO_x changes are 0, 1, 2, 4, 6, 8, and 10%. The contour intervals for the ozone changes are -1, -.5, -.2, -.1, 0, .1, .2, .5, and 1%.

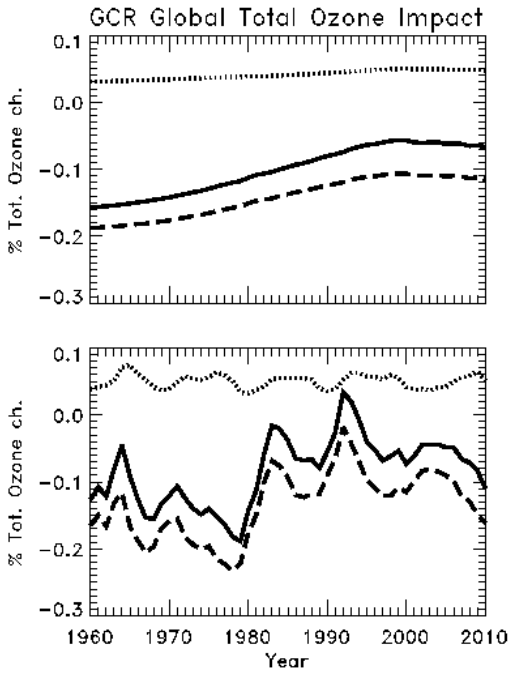

Figure 8~~7~~. GSFC 2-D model GCR-computed tropospheric column (dotted black), stratospheric column (dashed black), and total (solid black) AAGTO impacts over the 1960-2010 time period. The top plot shows the comparison of simulation *A1_GCR_GSFC* to *A_Base_GSFC*. The bottom plot shows the comparison of simulation *E_GCR_GSFC* to *E_Base_GSFC*.

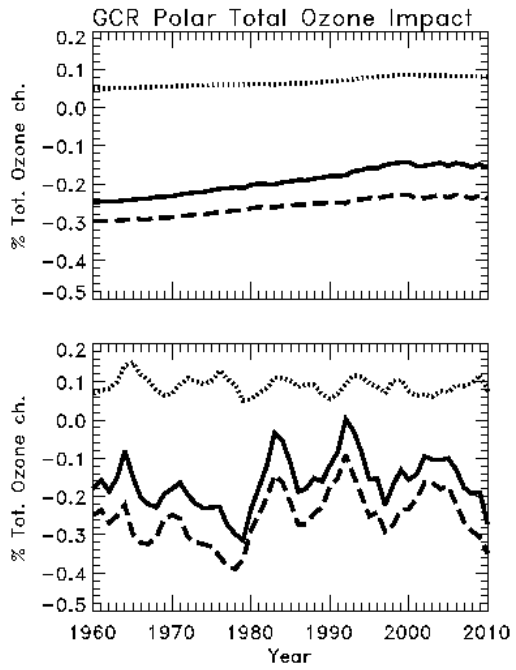

Figure 9. GSFC 2-D model GCR-computed impacts of annual average polar total ozone (AAPTO) between 1000 and 100 hPa (dotted black), between 100 and 1 hPa (dashed black), and for the entire troposphere and stratosphere, 1000 to 1 hPa, (solid black) over the 1960-2010 time period. The top plot shows the comparison of simulation A1_GCR_GSFC to A_Base_GSFC. The bottom plot shows the comparison of simulation E_GCR_GSFC to E_Base_GSFC.

Formatted: Left, Line spacing: 1.5 lines

Formatted: Font: (Default) Times New Roman, Not Italic

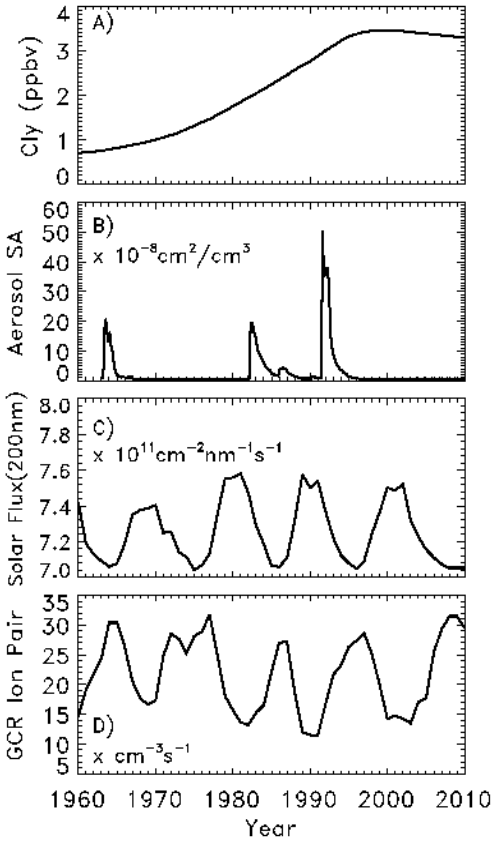

Figure 10~~8~~. Forcing used in the GSFC 2-D model over the 1960-2010 time period. These include: A) Background Total Chlorine (Cl_y, in ppbv); B) Aerosol Surface Area (SA) at 50 hPa and the Equator in 10^{-8} cm^2/cm^3; C) Solar Flux at 200 nm in 10^{11} $cm^{-2}nm^{-1}s^{-1}$; and D) GCR Ion Pair Production at 200 hPa and 90°S in $cm^{-3}s^{-1}$.

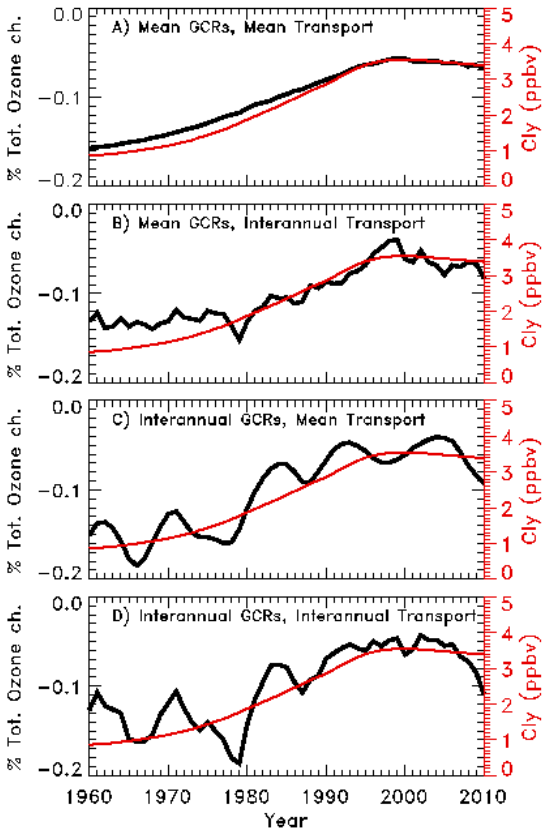

Figure 119. GSFC 2-D model GCR-computed AAGTO impacts (black lines) over the 1960-2010 time period. The Cl_y levels are also shown (red lines). The GSFC 2-D model comparisons include: A) Mean GCRs, Mean Transport (simulation *A1_GCR_GSFC* compared to *A_Base_GSFC*); B) Mean GCRs, Interannual Transport (simulation *B1_GCR_GSFC* compared to *B_Base_GSFC*); C) Interannual GCRs, Mean Transport (simulation *A2_GCR_GSFC* compared to *A_Base_GSFC*); and D) Interannual GCRs, Interannual Transport (simulation *B2_GCR_GSFC* compared to *B_Base_GSFC*).

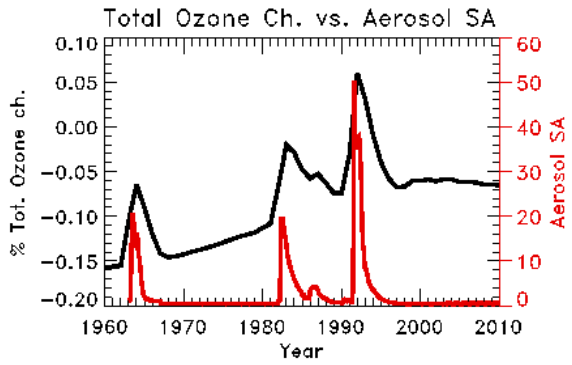

Figure 12~~0~~. GSFC 2-D model GCR-computed AAGTO impacts (black line) over the 1960-2010 time period (simulation *C_GCR_GSFC* compared to *C_Base_GSFC*). The Aerosol Surface Area (SA) at 50 hPa and the Equator is also shown (red lines), given in 10^{-8} cm^2/cm^3.

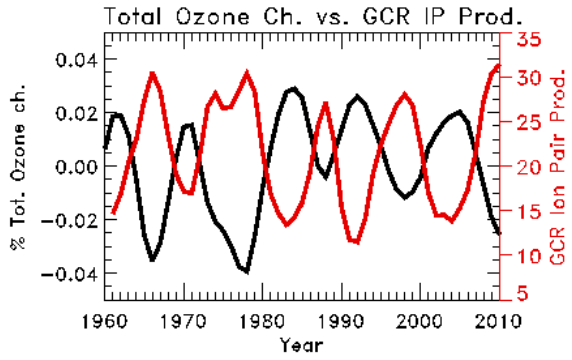

Figure 13~~1~~. GSFC 2-D model GCR-computed AAGTO change (black line) over the 1960-2010 time period caused by the interannual GCR variation. The global total ozone change shown in Figure 11~~9~~C is differenced from that shown in Figure 11~~9~~A. A two-year boxcar (running) average of the GCR Ion Pair Production (in $cm^{-3}s^{-1}$) at 200 hPa and 90°S with a one-year lag is also shown (red line).

Page 22: [1] Formatted **Jackman, Charles H. (GSFC-6140)** **2/18/2016 3:17:00 PM**

Font: (Default) Times New Roman, Not Italic

Page 22: [2] Formatted **Jackman, Charles H. (GSFC-6140)** **2/18/2016 3:17:00 PM**

Font: (Default) Times New Roman, Not Italic

Page 22: [3] Formatted **Jackman, Charles H. (GSFC-6140)** **2/18/2016 3:39:00 PM**

Font: (Default) Times New Roman, Not Italic